Articles in PresS. Am J Physiol Endocrinol Metab (June 27, 2017). doi:10.1152/ajpendo.00438.2015

Lipid remodelling and an altered membrane associated proteome may drive the differential effects of EPA and DHA treatment on skeletal muscle glucose uptake and protein accretion

Stewart Jeromson[1], Ivor Mackenzie[2], Mary K. Doherty[2], Phillip D. Whitfield[2], Gordon Bell[3], James Dick[3], Andy Shaw[1], Francesco Rao[4], Stephen P. Ashcroft[5], Andrew Philp[5], Stuart Galloway[1], Iain Gallagher[1], D. Lee Hamilton[1]†

1. Health and Exercise Sciences Research Group, University of Stirling, Stirling, UK, FK9 4LA.
2. Department of Diabetes and Cardiovascular Science, University of Highlands and Islands, Inverness, UK, IV2 3JH.
3. Institute of Aquaculture, University of Stirling, Stirling, UK, FK9 4LA.
4. Dundee Cell Products, Dundee Technopole, Dundee, UK, DD1 5JJ.
5. School of Sport, Exercise and Rehabilitation Sciences, University of Birmingham, Birmingham, UK, B15 2TT.

†Corresponding Author:
D. Lee Hamilton
Health and Exercise Sciences Research Group,
University of Stirling,
Stirling,
UK,
FK9 4LA

Running Title: Skeletal muscle lipid remodelling by EPA and DHA.

Abstract

In striated muscle, EPA and DHA have differential effects on the metabolism of glucose and differential effects on the metabolism of protein. We have shown that, despite similar incorporation, treatment of C_2C_{12} myotubes (CM) with EPA but not DHA improves glucose uptake and protein accretion. We hypothesized that these differential effects of EPA and DHA may be due to divergent shifts in lipidomic profiles leading to altered proteomic profiles. We therefore carried out an assessment on the impact of treating CM with EPA and DHA on lipidomic and proteomic profiles. FAME analysis revealed that both EPA and DHA led to similar but substantial changes in fatty acid profiles with the exception of arachidonic acid, which was decreased only by DHA, and DPA, which was increased only by EPA treatment. Global lipidomic analysis showed that EPA and DHA induced large alterations in the cellular lipid profiles and in particular, the phospholipid classes. Subsequent targeted analysis confirmed that the most differentially regulated species were phosphatidylcholines and phosphatidylethanolamines containing long chain fatty acids with 5 (EPA treatment) or 6 (DHA treatment) double bonds. As these are typically membrane associated lipid species we hypothesized that these treatments differentially altered the membrane-associated proteome. SILAC based proteomics of the membrane fraction revealed significant divergence in the effects of EPA and DHA on the membrane associated proteome. We conclude that the EPA specific increase in polyunsaturated long chain fatty acids in the phospholipid fraction is associated with an altered membrane associated proteome and these may be critical events in the metabolic remodelling induced by EPA treatment.

Keywords: cell signalling, fish oil, fatty acid, insulin, lipidomics, lipids

Introduction

Fatty acids play an important role in skeletal muscle metabolism, not only as substrates for oxidative phosphorylation or vital structural components of membranes but also as regulators of enzyme activities and signalling molecules (8). Furthermore, dysfunctions in the control of fatty acid metabolism can be an important factor in the aetiology of conditions such as insulin resistance and muscle atrophy (8). The lipid composition of skeletal muscle undergoes constant fluctuations and is reflective of dietary fat intake (6). There is strong evidence to suggest that the enrichment of skeletal muscle with omega-3 (n-3) fatty acids may have therapeutic benefits on muscle metabolism and function (14). Oral n-3 supplementation above the Reference Dietary Intake is known to result in significant incorporation of n-3 fatty acids into the skeletal muscle lipid pool (6, 13, 30).

Several n-3 supplementation studies in humans have observed beneficial effects ranging from an increased sensitivity to anabolic stimuli (43, 44) and muscle function (40, 45). Eight weeks n-3 supplementation improved the muscle protein synthetic response (MPS) to a hyperinsulinaemic amino acid infusion in both young (44) and elderly individuals (43). Furthermore, when taken alongside a resistance based exercise programme (12, 40) or in the absence of any strength training (45) n-3 fatty acids enhance strength and or physical function in the elderly. Concurrent with anabolic properties, n-3 FAs also display anti-catabolic effects. n-3 supplementation prevented muscle mass losses in burned guinea pigs (5) and protected against muscle mass loss during anti-neoplastic therapy in cancer patients (34). However, when combined in systematic reviews do not always show a beneficial effect on muscle mass during cancer treatment (39). Moreover n-3 FAs attenuated soleus atrophy in rodents that underwent 10 days of hind limb immobilization (55).

As well as effects on muscle protein metabolism there is building evidence to suggest that n-3 fatty acids may also modulate glucose metabolism. Current meta-analyses detect a neutral or small effect of n-3 FAs on measures of insulin sensitivity (4). However, there are several studies across a range of models utilizing higher doses of n-3s which support a role for n-3s in improving muscle mitochondrial function and glucose metabolism (23, 28, 35, 37, 47, 48). For instance, replacing 3.4% of the Kcals

with n-3 fatty acids on a high fat diet protects mice against declines in glucose tolerance during a 10-week high fat diet despite similar increases in body weight compared to high fat alone (28). Whereas supplementation studies in humans have not demonstrated a consensus (4), an interesting lipid infusion trial has shown n-3 fatty acids to be bioactive in humans with respect to glucose metabolism (46). More specifically, the addition of n-3 fatty acids to a lipid infusion of n-6 fatty acids attenuated the decline in insulin stimulated glucose disposal caused by n-6 infusion alone suggesting that the n-3 fatty acids have a protective effect on glucose metabolism in the presence of an n-6 overload (46).

Fish oil and n-3 supplements are a heterogeneous mixture of fatty acids of which eicosapentaenoic acid (EPA, 20:5) and docosahexaenoic acid (DHA 22:6) are thought to be the most biologically active. Due to many studies using a combination of EPA and DHA and varying ratios of each fatty acid it is difficult to assert whether EPA or DHA alone is causing the observed effects or if EPA and DHA work synergistically or antagonistically for that matter. The molecular mechanisms of n-3 action are still poorly understood. Work from Olefsky's lab suggests that GPR120 acts as a general n-3 receptor in macrophages and adipocytes that, when activated by n-3 fatty acids leads to increases in whole body insulin sensitivity by reducing inflammation (37). EPA has also been shown to antagonise the action of TNFα on C_2C_{12} myotube formation in a manner partially dependent on PPARγ (29). Additionally, EPA reduces the activation of Nuclear Factor-κappa Beta (NF-Kb) leading to a reduction in Muscle RING finger protein-1 (Murf-1) signalling, an important mediator of muscle atrophy in cultured myotubes (22). Furthermore, a follow up study employing both EPA and DHA demonstrated that DHA was more efficient in this mechanism than EPA (52). However, EPA has been shown to improve metabolic flexibility in response to changing substrate availabilities (21). EPA has also previously been shown to improve both basal and insulin stimulated glucose uptake in cultured myotubes (1). However, it remains to be seen whether DHA similarly improves glucose uptake in skeletal muscle. Despite the numerous similar intracellular effects and similar structure, EPA and DHA may have divergent physiological effects in skeletal muscle. EPA improves skeletal muscle protein metabolism while DHA has a non-significant effect (24). In other striated muscle models such as cardiomyocytes, EPA but not DHA increases glucose and fatty acid uptake despite

similar effects on cell signalling (18). In plasma both EPA and DHA reduced triacylglycerol (TAG) but only DHA modulates HDL (high density lipoprotein) and LDL (low density lipoprotein) particle size (53). Collectively these data suggest that in certain contexts, EPA and DHA can have differential biological effects.

The molecular mechanisms underpinning the divergent physiological effects of EPA vs DHA are currently under explored. However, differential remodelling of the lipid profile may partially explain the divergent physiological response observed between EPA and DHA. Currently studies attempting to address how n-3 fatty acids affect the lipidomic profile of skeletal muscle are limited. As expected n-3 intake leads to incorporation into the lipid pool of multiple tissues i.e. plasma, muscle, adipose tissue and liver with a significant proportion being directed towards phospholipid pools (7, 27, 30, 42-44). This incorporation is not limited to the plasma membrane and is also incorporated into subcellular organelles such as mitochondria (20). It is hypothesized that a primary driver of the effects of EPA and DHA is the displacement of arachidonic acid (AA) from membranes with studies from a range of models supporting this (27, 32, 42) while some *in vivo* human studies observe no change in total AA in the skeletal muscle lipid pool (30). However, this does not discount the possibility that AA might be displaced from specific lipid fractions. Multiple human studies have assessed the impact of n-3 supplementation on skeletal muscle phospholipid pool however the use of a heterogeneous mix of n-3 fatty acids precludes the ability to detect the isolated effects of EPA vs DHA on lipid profiles (6, 13, 30). Furthermore, into which skeletal muscle phospholipid fractions EPA and DHA are incorporated are poorly understood. In plasma phospholipids EPA and DHA induce a similar lipid profile yet EPA increased docosapentanoic acid (DPA 22:5 n-3) and a differential but non-significant increase in stearate acid (SA 18:0) (31). In smooth muscle cell phospholipids both EPA and DHA are heavily incorporated into the phosphatidylcholine (PC) fraction but EPA is divergently incorporated into the phosphatidylinositol (PI) and phosphatidylserine (PS) fraction while DHA is incorporated into the phosphatidylethanolamine (PE) fraction (33).

One of the main cellular fates for fatty acids is incorporation into complex lipid species and so it seems logical to hypothesize that the differential action of EPA and DHA may be due to differential

125 effects on the cellular lipidome. To date no study has characterised the impact of EPA and DHA
126 individually on lipidomic profiles in skeletal muscle. In this manuscript we demonstrate that the C_2C_{12}
127 cell line acts as a model in which EPA and DHA have differential effects on metabolism. We
128 followed these experiments by an extensive assessment of lipid changes hypothesizing that the
129 divergent effects of EPA and DHA are associated with differential regulation of the skeletal muscle
130 lipidome. The lipidomic profiling indicated that multiple membrane associated lipid species were
131 differentially altered by EPA and DHA treatments. We therefore hypothesized that the lipidomic
132 remodelling would be associated with remodelling of the membrane-associated proteome. SILAC
133 based proteomics of the membrane fraction indicated EPA and DHA differentially regulate the
134 membrane associated proteome. Therefore, the effects of EPA may be due to membrane associated
135 proteomic remodelling secondary to lipidomic remodelling of the membrane-associated lipids.

136

Materials and methods

Materials

All plasticware for tissue culture was purchased from fisher scientific (UK). Tissue culture media and sera were purchased from Invitrogen. Fatty acids EPA and DHA (>99%, liquid form) were purchased from Sigma Aldrich (Dorset, UK). $H^3$2-DG was purchased from Hartman Analytic. All solvents were LC-MS grade (Fisher Scientific, Loughborough, UK).

Cell culture

C_2C_{12} myoblasts were grown in Dulbecco's Modified Eagle Medium (DMEM) containing 20% fetal bovine serum and 1% penicillin/streptomycin and incubated at 37°C and 5% C02. Myoblasts were maintained at ~60% confluence. Differentiation was induced once confluence reached 80-90% by changing the media to differentiation media (DMEM supplemented with 2% horse serum and 1% Penicillin/Streptomycin) for 72 hours. Following 72 hours differentiation cells were treated with 50 µM EPA or 50 µM DHA pre-bound to 2% fatty acid free BSA for 72 hours before collection. As a control cells were treated with 2% fatty acid free (FAF) BSA for 72 hours before collection. Fatty acids were conjugated to 2% fatty acid free BSA in DM by constant agitation for 1 hour at 37°C. Following treatment cell pellets were collected following 3 washes in 2% FAF BSA in PBS and centrifuged at 800 rpm for 4 minutes, excess liquid was removed and pellets were frozen in liquid nitrogen and stored at -80°C until further analysis.

FAME analysis

Total lipids were extracted by homogenising in 20 volumes of chloroform/methanol (2:1 v/v). Total lipids were prepared according to the method of Folch et al. (17) and non-lipid impurities were removed by washing with 0.88% (w/v) KCl. The weight of lipids was determined gravimetrically after evaporation of solvent and overnight desiccation under vacuum. Fatty acid methyl esters (FAME) were prepared by acid-catalysed transesterification of total lipids according to the method of Christie et al. (35). Extraction and purification of FAME was performed as described by Ghioni et al. (36). FAME were separated by gas-liquid chromatography using a ThermoFisher Trace GC 2000

(ThermoFisher, Hemel Hempstead, UK) equipped with a fused silica capillary column (ZBWax, 60m x 0.25 μm x 0.25 mm i.d.; Phenomenex, Macclesfield, UK) with hydrogen as carrier gas and using on-column injection. The temperature gradient was form 50 to 150^{o}C at 40^{o}C/min and then to 195^{o}C at 1.5^{o}C/min and finally to 220^{o}C at 2^{o}C/min. Individual methyl esters were identified by reference to published data (Ackman, 1980). Data were collected and processed using the Chromcard for Windows (version 2.00) computer package (Thermoquest Italia S.p.A., Milan, Italy). All experiments were carried in duplicate from 4 independent experiments. Data were represented as fold change from the respective BSA control condition, logged to $\log_2$ and significance was determined by t-test and corrected for false discovery rate.

Global lipidomic analysis of C_2C_{12} myotubes

Lipid extraction was performed according to the method described above. The lipids were analysed by liquid chromatography-mass spectrometry (LC-MS) using a Thermo Exactive Orbitrap mass spectrometer (Thermo Scientific, Hemel Hempstead, UK), equipped with a heated electrospray ionization probe and coupled to a Thermo Accela 1250 UHPLC system. All samples were analysed in both positive and negative ion mode over the mass to charge (m/z) range 200-2000. The lipids were separated on to a Thermo Hypersil Gold C18 column (1.9 μm, 2.1mm x 100 mm,). Mobile phase A consisted of water containing 10 mM ammonium formate and 0.1% (v/v) formic acid. Mobile phase B consisted of 90:10 isopropanol/acetonitrile containing 10 mM ammonium formate and 0.1% (v/v) formic acid. The initial conditions for analysis were 65%A/35%B. The percentage of mobile phase B was increased to 100% over 10 min and held for 7 minutes before re-equilibration with the starting conditions for 4 minutes. The raw LC-MS data were processed with Progenesis QI v2.0 software (Non-linear Dynamics, Newcastle, UK) and searched against LIPID MAPS (www.lipidmaps.org) and the Human Metabolome Database (http://www.hmdb.ca/) for identification. All experiments were carried out in duplicate from three independent experiments.

Phospholipid profiling of C_2C_{12} myotubes

In order to assess the incorporation of EPA and DHA into cellular phospholipids the lipid extracts from C_2C_{12} myotubes were analysed by electrospray ionisation-tandem mass spectrometry (ESI-MS/MS). All analyses were performed using a Thermo TSQ Quantum Ultra triple quadrupole mass spectrometer equipped with a heated electrospray ionization probe. Samples were directly infused into the ion source at a flow rate of 5 µL/min. Phosphatidylcholine, lysophosphatidylcholine and sphingomyelin species were identified by precursor scanning for mass to charge ratio (m/z) 184 in positive ion mode. Phosphatidylethanolamine and lysophosphatidylethanolamine species were identified by neutral loss scanning for m/z 141 in positive ion mode. Phosphatidylserine species were identified by neutral loss scanning for m/z 87 in negative ion mode. Phosphatidylinositol species were identified by precursor scanning for m/z 241 in negative ion mode. The data were expressed as a percentage composition of the relevant phospholipid fraction.

Glucose uptake

C2C12 myotubes, were exposed to 50µM EPA or 50µM DHA pre-bound to 2% fatty acid free BSA or 2% fatty acid free BSA as a control for 48 h before a 2 h serum-starve. Following the 2 h serum starve cells were exposed to insulin (100 nmol/l) or vehicle control for 30 mins. Myotubes were incubated (12 min) with 10 µmol/l 2-deoxy-D-[3 H]glucose (2DG; 24.4 kBq/ml; Hartman Analytic) at 20°C. Non-specific uptake was determined using 10 µmol/l cytochalasin B (Sigma–Aldrich). After lysis, cell-associated radioactivity was measured (Beckman, High Wycombe, UK; LS 6000IC scintillation counter), and protein was quantified using the Bradford reagent. Data represented are the average of 6 independent experiments carried out in duplicate.

Mitochondrial function

C2C12 myotubes, were exposed to 50µM EPA or 50µM DHA pre-bound to 2% fatty acid free BSA or 2% fatty acid free BSA as a control for 48 h. Following 48 h in the respective treatments cells were degassed and exposed to a mito-stress test in the Seahorse cellular respiration analyser as previously described (16).

Muscle protein synthesis and muscle protein breakdown

Protein degradation was assessed by the quantification of the released L-[2,4,^{3}H] phenylalanine into the culture media. Following 4 days of differentiation myotubes were incubated with medium containing 2.5 µCi L-[2,4,^{3}H] phenylalanine/ml and the label was maintained for 24 hours in order to label long lived proteins. Following the pulse the cells were washed 2x in PBS and incubated in cold chase media (DMEM + 2mM L-phenylalanine) for 3 hours to allow for degradation of short lived proteins. Myotubes were then treated with either 50 µM EPA/DHA bound to 2% FAF-BSA or 2% FAF-BSA alone for 24 hrs. Following treatment an aliquot of the media was removed and radioactivity released was assessed by scintillation counting. The remaining myotubes were then thoroughly washed with ice cold saline (0.9%) and lysed with 50mM NaOH + 1% SDS for a minimum of 30 mins at room temperature. Residual radioactivity in cell lysates was then assessed by scintillation counting. Total radioactivity was calculated as the sum of the L-[2,4,^{3}H] phenylalanine released into the media and the residual cell retained L-[2,4,^{3}H] phenylalanine. Protein breakdown is presented as the fraction of the total incorporated L-[2,4,^{3}H] phenylalanine released into the media.

Basal protein synthesis was assessed by the incorporation of L-[2,4,^{3}H] phenyalalnine into peptide chains. Following differentiation, myotubes were treated with either 50 µM EPA/DHA bound to 2% FAF-BSA or 2% FAF-BSA alone for 24 hrs. At the end of the treatment period the media was removed and DMEM containing 1µCi L-[2,4^{3}H] phenylalanine (0.5 µCi/ml) was added for 180 mins. The reaction was stopped by 2x washes in ice cold saline (0.9%) before 3x washes with Tricholoroacetic acid (TCA) (10%) to remove any unincorporated tracer. Residual TCA was then removed by rinsing cells with methanol and plates left to dry. Myotubes were then lysed in 50mM NaOH + 1% SDS for a minimum of 30 minutes. An aliquot was collected for liquid scintillation counting to assess ^{3}H incorporation into proteins and the remaining lysate was used to determine protein content by the DC protein assay. Protein synthesis is presented as counts per minute/µg of protein.

Protein content

Protein content following 72 h treatment with 50μM EPA or 50μM DHA pre-bound to 2% fatty acid free BSA or 2% fatty acid free BSA as a control was determined by multiplying the concentration of the supernatant [as determined using the bicinchoninic acid protein assay according to the manufacturer's instructions (Sigma Aldrich, UK)] by the total volume of supernatant collected from a 6 well plate. Data are representative of 5 independent experiments carried out in triplicate.

Cell processing

Cell lysates were collected from 6 well plates by scraping on ice in RIPA buffer [50 mmol/l Tris·HCl pH 7.5, 50 mmol/l NaF, 500 mmol/l NaCl, 1 mmol/l sodium vanadate, 1 mmol/l EDTA, 1% (vol/vol) Triton X-100, 5 mmol/l sodium pyrophosphate, 0.27 mmol/l sucrose, and 0.1% (vol/vol) 2-mercaptoethanol and Complete protease inhibitor cocktail (Roche)] followed by snap freezing on liquid nitrogen. For preparation for western blotting samples were thawed and debris was removed by centrifugation at 4°C for 15 min at 13,000 g. The supernatant was then removed, and protein concentration was determined using the bicinchoninic acid protein assay according to the manufacturer's instructions (Sigma Aldrich, UK).

Western blotting

For WB, 100μg of supernatant was made up in Lamelli sample buffer, and 15 μg of total protein was loaded per well and run at 150 V for 1 h 15 min. Proteins were then transferred onto Whatman Immunobilon Nitrocellulose membranes (Fisher Scientific, Loughborough, UK) at 30 V overnight on ice. Membranes were blocked in 3% BSA-Tris-buffered saline (containing vol/vol 0.1% Tween 20) for 1 h at room temperature, followed by incubation in primary antibodies [PKBthr308 (#2965) or total PKB (#4691) GLUT 1(Santa cruz, sc-7903), GLUT4 (#2213S), Hexokinase 1 (#2204S), Hexokinase 2 (#2867S), Mito profile (abcam, #ab110413) (New England Biolabs unless stated)] at 4°C overnight. Membranes underwent three 5 min washes in TBST followed by incubation in the appropriate secondary antibodies [secondary horseradish peroxidase conjugated antibody was purchased from ABCAM (#6721)] for 1 h at room temperature. Membranes were again washed three

times for 5 min followed by incubation in enhanced chemiluninescence reagent (BioRad, Herts, UK). A BioRad ChemiDoc (Herts, UK) was used to visualize and quantify protein expression. Phospho-PKB was normalized to the corresponding total protein. Data are representative of 3 independent experiments carried out in duplicate.

Membrane proteome

Proteins associated with membranes were assessed using the SILAC proteomic method (38). C_2C_{12} myoblasts were grown in Dulbeccos' modified eagles medium (DMEM) supplemented with 20% dialysed (10 kKDa) foetal bovine serum plus labelled amino acids lysine and arginine in a humidified atmosphere of 37°C and 5% CO2. Cells intended to act as the control group were grown in with unlabelled lysine and arginine (light), the EPA treatment group were grown in R6K4 media (l-arginine-13C6 hydrochloride, l-lysine-4,4,5,5-d4 hydrochloride[medium]) while the DHA treatment group were grown with R10K8 containing media (l-arginine-13C6, 15N4 hydrochloride, l-lysine-13C6,15N2 hydrochloride [Heavy]). The use of combined labelled arginine and lysine ensures that nearly all peptides will contain a label after tryptic digestion. Cells were allowed to grow for at least 6 population doublings to ensure full incorporation of labelled amino acids. We observed that use of dialysed sera and labelled media did not affect doubling time, cell morphology or differentiation capacity. Upon reaching 90-100% confluence the media was replaced with DMEM containing 2% dialysed donor horse serum (10 kDa) to induce differentiation. After 3-4 days of differentiation, myotubes were treated with either control, 50μM EPA or 50 μM DHA for 72 hours. For membrane proteome analysis, membranes were isolated using the Thermo scientific Mem per plus protein membrane extraction kit. The membrane proteome was assessed by LC-MS/MS.

Mass spectrometry

The resulting peptides were fractionated using an Ultimate 3000 nanoHPLC system in line with an Orbitrap Fusion Tribrid mass spectrometer (Thermo Scientific). In brief, peptides in 1% (vol/vol) formic acid were injected onto an Acclaim PepMap C18 nano-trap column (Thermo Scientific). After washing with 0.5% (vol/vol) acetonitrile 0.1% (vol/vol) formic acid peptides were resolved on a 250 mm × 75 μm Acclaim PepMap C18 reverse phase analytical column (Thermo Scientific) over a 150

296 min organic gradient, using 7 gradient segments (1-6% solvent B over 1min., 6-15% B over 58min.,
297 15-32%B over 58min., 32-40%B over 5min., 40-90%B over 1min., held at 90%B for 6min and then
298 reduced to 1%B over 1min.) with a flow rate of 300 nl min^{-1}. Solvent A was 0.1% formic acid and
299 Solvent B was aqueous 80% acetonitrile in 0.1% formic acid. Peptides were ionized by nano-
300 electrospray ionization at 2.0 kV using a stainless steel emitter with an internal diameter of 30 μm
301 (Thermo Scientific) and a capillary temperature of 275°C.

302 All spectra were acquired using an Orbitrap Fusion Tribrid mass spectrometer controlled by Xcalibur
303 2.1 software (Thermo Scientific) and operated in data-dependent acquisition mode. FTMS1 spectra
304 were collected at a resolution of 120 000 over a scan range (m/z) of 350-1550, with an automatic gain
305 control (AGC) target of 300 000 and a max injection time of 100ms. Precursors were filtered using an
306 Intensity Range of 1E4 to 1E20 and according to charge state (to include charge states 2-6) and with
307 monoisotopic precursor selection. Previously interrogated precursors were excluded using a dynamic
308 window (40s +/-10ppm). The MS2 precursors were isolated with a quadrupole mass filter set to a
309 width of 1.4m/z. ITMS2 spectra were collected with an AGC target of 20 000, max injection time of
310 40ms and CID collision energy of 35%.

311 **Quantification and bioinformatics analysis**

312 The raw mass spectrometric data files obtained for each experiment were collated into a single
313 quantitated data set using MaxQuant (version 1.2.2.5) (10) and the Andromeda search engine software
314 (11). Enzyme specificity was set to that of trypsin, allowing for cleavage N-terminal to proline
315 residues and between aspartic acid and proline residues. Other parameters used were: (i) variable
316 modifications, methionine oxidation, protein N-acetylation, gln → pyro-glu, Phospho(STY); (ii) fixed
317 modifications, cysteine carbamidomethylation; (iii) database: target-decoy human MaxQuant
318 (ipi.HUMAN.v3.68); (iv) heavy labels: R6K4 and R10K8; (v) MS/MS tolerance: FTMS- 10ppm ,
319 ITMS- 0.6 Da; (vi) maximum peptide length, 6; (vii) maximum missed cleavages, 2; (viii) maximum
320 of labeled amino acids, 3; and (ix) false discovery rate, 1%. Peptide ratios were calculated for each
321 arginine- and/or lysine-containing peptide as the peak area of labeled arginine/lysine divided by the
322 peak area of nonlabeled arginine/lysine for each single-scan mass spectrum. Peptide ratios for all

arginine- and lysine-containing peptides sequenced for each protein were averaged. Data is normalised using 1/median ratio value for each identified protein group per labelled sample.

Statistics

Statistical analyses were carried out in Graphpad Prism with ANOVA followed by Tukey's HSD test. For FAME analyses data were assessed in R statistical packages and tested by t-test and corrected by false discovery rate. Statistical significance was determined with a $p<0.05$. The global lipidomic data sets were subjected to principal component analysis (PCA) and orthogonal projection latent structure-discriminant analysis (OPLS-DA) with Pareto scaling using SIMCA-P v13.0 software (Umetrics, Umea, Sweden). The OPLS-DA models were validated by using the internal cross-validation function. Membrane protein abundance was considered altered if fold change was lower than 0.75 or greater than 1.25. Enrichment of biological processes was determined using gene ontology, using the whole genome of Mus musculus as a background reference list.

Results

EPA and DHA substantially increase the abundance of omega-3 species but have differential effects on individual omega-3 fatty acids.

After exposure to 50uM EPA or DHA for 72 hrs C_2C_{12} myotubes were collected for FAME analysis to determine lipid profiles. EPA and DHA significantly increased total omega-3 fatty acid content from baseline values (EPA; 951 ± 81% p=0.0014, DHA; 750 ± 56% p=0.0009) with no significant difference detected between EPA and DHA treatment (p=0.115) (**Figure 1)**. The changes in omega-3 abundance are a result of differential shifts in specific omega-3 fatty acids caused by EPA or DHA treatment. The increase in omega-3 content by DHA is a result of accumulation of mainly DHA [22:6 n-3, 3050% ± 310% (**Figure 5**)]. While, incubation of myotubes with EPA results in the accumulation of EPA [(20:5 n-3), 1630% ± 23.38] and DPA [(22:5 n-3), 1318% ± 199.8%] **(Figure 5)**. These data suggest that EPA is elongated to DPA whilst DHA remains largely unmodified.

EPA and DHA have differential effects on skeletal muscle glucose uptake.

Insulin stimulated 2-deoxy-glucose (2DG) uptake was determined after 48 h in either EPA or DHA. EPA treatment significantly increased both basal and insulin stimulated 2DG uptake indicating that EPA treatment increases the capacity for glucose uptake (**Figure 2A**). DHA did not have any significant effects on 2DG uptake (**Figure 2A**). The observed changes in 2DG uptake did not appear to be related to any change in insulin stimulated PKB phosphorylation as phospho-blot analysis revealed that insulin stimulated PKB phosphorylation was the same between treatments and controls (**Figure 2B**). In addition EPA/DHA treatment did not appear to affect GLUT1 or GLUT4 expression (**Figure 1C**), nor did they appear to affect the expression of Hexokinase 1 or Hexokinase 2 (**Figure 1D**).

EPA and DHA treatment does not alter mitochondrial respiration.

As no changes in glucose transporters were detected we next assessed whether changes in mitochondrial oxygen consumption may explain the increase in glucose uptake following EPA treatment. C_2C_{12} myotubes were treated with 50uM EPA or DHA for 24 hours. Following treatment

multiple inhibitors/uncouplers (Oligomycin, FCCP, rotenone/anitmycin A) were used to probe various parameters of mitochondrial function using the seahorse XF mito stress test. A two way ANOVA found a significant interaction between oxygen consumption and inhibitor compound, indicating the successful manipulation of mitochondrial function (**Figure 3A**). However, fatty acid treatment did not lead to changes in cellular oxygen consumption on any parameter measured (**Figure 3A**). Consistent with the lack of changes in mitochondrial function, there were no alterations in the abundance of ATP synthase and UCQR2 (Complex V and Complex III respectively) (**Figure 3B/C).**

EPA enhances protein accretion through a reduction in protein breakdown while DHA has a neutral effect

After a 72 hour incubation with EPA or DHA, myotubes were collected in order to determine total protein content. When myotubes were incubated with EPA total protein content was enhanced while incubation with DHA had a neutral effect (**Figure 4C**). Protein balance is determined by the balance between synthesis and breakdown of proteins. Thus, the observed protein accretion may be reflected in changes in either protein synthesis or breakdown. In order to understand the mechanisms underlying the changes in protein content we directly assessed protein synthesis and breakdown and related signalling processes. Neither fatty acid had any effect on basal protein synthesis after a 24-hour incubation (**Figure 4A**). Anabolic signalling assessed by the phosphorylation status of mTOR, P70S6K1 and 4E-BP1 were not different between groups, corresponding with lack of changes in protein synthesis (**Figure 4E/F**). EPA reduced protein breakdown compared to both the vehicle and DHA treatments (**Figure 4B**). No changes were detected in the level of ubiquitin tagged proteins (**Figure 4D/F**).

EPA treatment differentially regulates DPA levels whilst DHA treatment differentially regulates arachidonic acid levels. As previously mentioned, incubation of C2C12 with 50 μM EPA or 50 μM DHA led to substantial cellular incorporation of total omega-3 fatty acids (**Figure 1A**). This was associated with the above mentioned physiological changes. In order to determine the potential mechanisms by which these effects occur we determined via FAME analysis the fatty acid changes responsible for the increase in total n-3 levels in the cells treated with EPA/DHA. In order to clearly

distinguish differential fatty acid shifts we presented the complete fatty acid profiles as fold change [(log2) **Figure 5**]. The most clearly differentiated fatty acid is DPA (22:5 n3) which demonstrates a significant 1318 ± 200% increase with EPA treatment whilst DHA treatment induces a 17.83 ± 17.37% decrease in DPA content. Additionally there is a trend (p=0.06) for EPA treatment to increase the DHA content of the cells (37.11 ± 12.62%) suggesting that only a small proportion of the EPA is converted to DHA. Surprisingly arachidonic acid (20:4 n6) was only significantly decreased by DHA treatment (-22.35 ± 3.174%) and remained unaffected by EPA treatment. Intriguingly we also observed that both EPA and DHA increased the content of the saturated fatty acid palmitate (PA 16:0) **(Figure 5**). In order to build a more complete picture of the impact of EPA and DHA on the lipidome we proceeded with a global lipidomics assessment.

Global lipidomics reveals that EPA and DHA treatments induce substantial divergence in the lipidome. Lipid extracts of cells treated with BSA (control), EPA or DHA were analysed by LC-MS in positive and negative ion modes, processed and subjected to multivariate data analysis. PCA highlights any natural clustering or separation within a data set and thereby enables similarities or differences between study groups to be explored. The PCA scores plots of both the positive and negative ion data sets revealed that EPA and DHA supplementation caused a substantial divergence in the lipidome, effectively segregating control and treated cells (**Fig. 6A and 6B**). Having established the existence of clustering behaviour between the sample cohorts more powerful multivariate methods were used to characterise the specific lipid changes responsible for the observed shift in the lipidome of the EPA and DHA treated myotubes. The OPLS-DA scores plots and associated 'S' plots of the positive ion data are shown in **Fig. 7A and 7B**. The results indicated that many of the key discriminating lipids associated with EPA and DHA treatment were phospholipids and in particular molecular species of PC and PE.. In EPA treated cells elevations in PC and PE species containing both 20:5 and 22:5 fatty acids (in agreement with FAME analysis) were observed, whereas there were relative increases in the abundance of phospholipid species with a 22:6 fatty acid in DHA treated cells. The analysis also revealed that both EPA and DHA treatments also resulted in an elevation of PC 32:0, a saturated species. DHA was also found to be incorporated into a number of triglyceride

species (see supplemental). In order to fully understand the impact of EPA and DHA treatment we followed up these experiments through the targeted analysis of the myotube phospholipids.

Targeted phospholipid analysis reveals that EPA and DHA increase the fraction of lipid species containing long chains and 5 or more double bonds at the expense of shorter chain, less saturated species. ESI-MS/MS was utilised to characterise the profiles of myocyte phospholipid classes. Representative mass spectra of PC and PE are shown in **Figure 8A and 8B**. The general trends (**Figure 9**) in both EPA and DHA were similar with the displacement of shorter chain in apparent preference for longer chain highly unsaturated fatty acids. However, the magnitude of change for these displacements was often higher with DHA. There was no evidence of alterations in the profile of sphingomyelin species in response to fatty acid treatments. ESI-MS/MS analysis of PS and PI was also performed however the low signal intensities of these lipids did not permit a robust quantification. Interestingly EPA and DHA supplementation led to a higher abundance of phospholipid species containing saturated fatty acids. For instance DHA induced an increase in PC (32:0) and lysophosphatidylethanolamine (LPE) (16:0), whilst EPA induced an increase in PC (32:0,) LPC (16:0), (18:0) and LPE (18:0). It is therefore evident that in spite of significant increases in saturated fatty acids in these EPA and DHA treatment still improve or maintain glucose uptake respectively.

Altered composition of phospholipids is associated with altered membrane associated proteomic profiles.

As the lipidomic remodelling indicated substantial changes induced by n-3 treatment in the membrane associated lipid species we carried out SILAC based proteomics profiling of the membrane fraction to assess if the lipid remodelling altered the proteins in the membrane fraction. Over 3000 proteins associated with the membrane compartment were identified in the SILAC screen. These results were filtered down to 625 proteins (see supplemental) with a coefficient of variance $\leq$ 5% to describe consistent changes in membrane abundance. Proteins were considered enriched or reduced in the membrane with a fold change cut off of 0.25. Proteins similarly affected by EPA and DHA were removed from analysis. Proteins with altered abundance were then subject to gene ontology analysis

443 for biological processes (see supplemental). Membrane proteins altered by EPA were associated with
444 protein folding (p = 4.76E-03). Additionally, these proteins were subjected to String analysis which
445 revealed that these proteins were highly likely to interact with eachother (Figure 10B). EPA also
446 increased Calumenin in the membrane fraction (1.34 fold). Interestingly, Calumenin plays a role in
447 calcium sensitive protein folding (49). DHA altered proteins associated with a number of processes,
448 primarily related to oxidative metabolism and ribosomal formation (see table 1). Further examination
449 of ribosomal proteins revealed that DHA induced the significant reduction in ribosomal proteins
450 associated with both small and large subunits at the membrane (Figure 10C). Conversely, EPA
451 induced a small increase in ribosomal proteins (**Figure 10C**).

452

Discussion

This study is the first to carry out a comprehensive analysis of the lipidomic profiles of a skeletal muscle cell line in response to two differentially bioactive n-3 fatty acids. Furthermore, it is the first study, to our knowledge, to combine this with a profile of the membrane associated proteome. We clearly demonstrate the differential metabolic activities of EPA vs DHA in the C_2C_{12} skeletal muscle cell line and provide data demonstrating the differential impact that EPA and DHA have on the skeletal muscle lipidome. Our data suggests that the bioactivity of EPA may be due to its preferential incorporation (and possibly elongation to DPA) into the phospholipid fraction where it substantially alters the long chain polyunsaturated fatty acid composition of major phospholipid classes. Likely secondary to the alterations in membrane associated phospholipids we see an altered membrane associated proteome. These changes in the membrane lipid-protein composition may be a key driver for the metabolic effects of n3 fatty acids.

Similar to previous cell culture based studies (1, 21), we show that EPA has a positive effect on glucose uptake. Both basal and insulin stimulated muscle glucose uptake were improved by EPA but not DHA. The increase in glucose uptake appears to be independent of changes in PKB signalling as measured by phosphorylation status which suggests that enhanced proximal insulin and possibly PKB signalling are not part of the mechanism of action. Furthermore, there was no significant change to the expression of the glucose transporters GLUT1/4, hexokinase1/2 or the mitochondrial enzymes UQCRC2 and ATP-synthase. Nor was there any significant change in mitochondrial function as assessed by the mitochondrial stress test. These data are difficult to consolidate, however, we hypothesize that the mechanism of action of EPA on glucose uptake may be dependent less upon changes in protein expression and more dependent upon protein localisation perhaps improving the functional coupling of glucose metabolism enzymes.

In addition to the EPA induced improvements in glucose uptake we also noted a significant improvement in protein accretion with EPA treatment, while DHA showed no significant effect. To determine the mechanism by which cells treated with EPA accumulate more protein we assessed

muscle protein synthesis and muscle protein breakdown. While Kamolrat et al (24) observed enhanced leucine stimulated MPS following EPA treatment, we detected no significant changes in basal muscle protein synthesis or the phosphorylation of anabolic signalling markers. Instead, we determined that the effect of EPA on protein accretion was likely driven by an ~10% reduction in muscle protein breakdown. Analysis of global ubiquitination via western blotting indicates that the reduction in muscle protein breakdown may not be driven by a change in the activity of the ubiquitin system. Rather, it may be driven by reduced lysosomal degradation (9). In saying that we must concede however, that a 10% reduction in ubiquitin driven protein breakdown would be challenging to detect via western blotting.

In an effort to determine the molecular mechanism of action of EPA on skeletal muscle glucose uptake and protein accretion we tested the hypothesis that EPA and DHA treatments would induce significant lipid remodelling leading to remodelling of the cellular proteome. We found that while the total n-3 content was similar between treatments, EPA resulted in a larger variation in lipid species accumulating mainly as EPA and DPA and to a lesser extent DHA while DHA treatment mainly resulted in DHA accumulation with a decrease in DPA and a limited retro-conversion to EPA. The main differentially regulated fatty acids were DPA, increased in EPA and decreased in DHA, while only DHA decreased AA. Interestingly DPA accumulated to a similar extent as EPA [1630% (EPA) vs 1318% (DPA)], findings consistent with previous literature in other tissues (2, 26). Given that DPA increased to a similar extent to EPA we are unable to determine whether it is EPA or DPA that is the main driver behind the metabolic effects observed. These data suggest that upon intake into the cell EPA is elongated to DPA and to a lesser extent DHA. The elongation of EPA to DPA but not DHA may be explained by the differential affinities of the desaturases and elongases involved in fatty acid metabolism. In the n-3 pathway elovl2 catalyzes the conversion of EPA → DPA → 24:5 n-3, the precursor to DHA. However, increasing EPA concentrations is known to lower the saturation point in the conversion of DPA → 24:5 n-3 which may play a role the accumulation of DPA without being further metabolised to DHA (19). Our data indicate that one of the primary fates of EPA and DHA was incorporation into the phospholipid fraction. In the global lipidomics screen we found EPA or

DPA containing lipid species associated with the phospholipid pool whilst DHA containing species were often associated with the TAG pool whilst EPA containing species were rarely associated with the TAG pool (see supplemental spread sheet). Fatty acids in the TAG pool are stored in discrete lipid droplets and therefore may be less metabolically active than the phospholipids associated with the membranes. This differential incorporation into the various lipid pools may partially explain the beneficial metabolic effects of EPA.

The potential relevance of DPA as a mediator of many of the physiological effects of n-3 supplementation is beginning to be further understood. DPA more potently inhibits platelet aggregation than EPA or DHA (3) as well as more potently stimulating endothelial cell migration than EPA or DHA (25). In macrophages EPA is a known inhibitor of the cyclooxygenase pathway and elongation to DPA is an important factor in this inhibition (36). We would suggest that the elongation of EPA to DPA seen in our study may also have important physiological roles in the increase in skeletal muscle glucose uptake by EPA. As with the global lipidomic analysis we observed the incorporation of long chain PUFAs into phospholipid species mainly at the expense of specific SFAs and MUFAs, however some specific SFAs were increased by both EPA and DHA. We identified multiple differentially regulated phospholipid species across PE, PC, LPE and LPC classes. In the EPA treated group a number of species were enriched by long chain PUFAs with 5 or more double bonds in addition to a number of EPA or DPA containing phospholipids in the PC and PE, fractions In comparison, the DHA treated group increased the long chain PUFA containing phospholipids but did not increase or increase as much as EPA the content of species containing 22:5 or 40:5. Interestingly, with DHA treatment there was a trend for an increase in the palmitate containing lyso-PE content above that of control and EPA. Additionally, while it appears that many phospholipids containing saturated fatty acids are displaced in favour of polyunsaturated containing phospholipids we observe a rise in PC (32:0) with both EPA and DHA, which may reflect the rise in palmitate observed with FAME analysis. Incorporation of PUFAs into phospholipids is known to increase membrane fluidity and we speculate that this increase may be a compensatory mechanism to maintain a base level of membrane rigidity.

533 An attractive mechanism for the differential effects of EPA and DHA may lie in the reduced
534 production of different inflammatory eicosanoids. However, only DHA reduced the total amount of
535 AA. Additionally, the displacement of phospholipids alongside a lack of inflammatory stimulus
536 suggests it is unlikely that this would mediate the metabolic differences seen in this model. The G
537 protein coupled receptor GPR120 has previously been identified as a general n-3 sensor in a number
538 of tissues except skeletal muscle that elicits potent anti-inflammatory and consequently insulin
539 sensitizing effects (37). To our knowledge no such receptor exists in skeletal muscle that can
540 discriminate between EPA and DHA deeming it unlikely that the observed differential effects are
541 mediated by EPA or DHA through specific receptor activated signalling.

542 Phospholipid species are not merely inert structural components of cellular membranes and their
543 various roles in intracellular processes are beginning to be further understood. PS and PE are related
544 phospholipid species found predominantly in the inner membrane and contribute to the membrane
545 targeting and activation and modification of protein kinases [as reviewed (51)]. It has also previously
546 been seen that the lyso-PC, a hyrdrolyzed form of phospholipid, stimulated adipocyte glucose uptake
547 in a manner dependent upon chain length and saturation of the acyl group (54). We observed an
548 incorporation of long chain PUFAs (possibly EPA and DPA) into the PC, PS, PE and certain lyso-PL
549 species and therefore cannot discount that the change in acyl chain length and unsaturation level alters
550 the function of these PL species and leads to an increase in glucose uptake through a currently
551 unknown mechanism. Because, the lipid composition of the membrane can alter the targeting of
552 various proteins to the membrane (50, 51) we speculated that part of the mechanism of action of EPA
553 might be via a change in the composition of the membrane associated proteome. To test this theory
554 we carried out a 3 way SILAC experiment on the membrane fractions of cells treated with vehicle,
555 EPA or DHA.

556 Our SILAC experiment illustrated the proof of concept that the incorporation of EPA and DHA into
557 phospholipid species was associated with the alteration of proteins interacting with the membrane
558 compartment. There are a number of mechanisms by which proteins can bind to the membrane which
559 are influenced by the fatty acid composition of the lipid bilayers (50, 51). Gene ontology analysis

indicated that proteins associated with protein folding at the membrane were overrepresented following EPA incorporation. There is experimental evidence that a number of the proteins identified with this process interact, as probed by the STRING database. Furthermore, analysis of ribosomal proteins indicated a small but significant shift of ribosomal proteins towards the membrane fraction in EPA treated cells. Since the endoplasmic reticulum is a membranous structure these data suggest that EPA is increasing the content of ribosomes at the ER. This shift in ribosomes towards the ER could lead to improved fidelity of protein production as the ER is key to protein quality control (15). We propose a mechanism in which protein folding is enhanced, thereby enhancing the fidelity with which proteins are synthesised thereby reducing protein breakdown leading to increased protein accretion. Further experimental work is needed to confirm this hypothesis since mis-folded proteins tend to be degraded by the ubiquitin-proteasome system (9) and our data indicated that global ubiquitination was not reduced by EPA. By comparison, DHA caused a striking reduction in the abundance of a number of ribosomal proteins with the membrane fraction. If future work confirms that total ribosomal content is unchanged with these conditions then these data would indicate an increase in cytosolic ribosomes. This differential shift in ribosomal compartmentalisation may indicate a shift in protein expression profiles. Proteins that enter the secretory pathways or integral membrane proteins are synthesised in the ER while other proteins are translated in the cytosolic ribosome pool (41).

DHA also altered the abundance of proteins involved in ATP coupled proton transport and acetyl-CoA metabolism. The proteins identified with ATP synthesis coupled transport were mainly downregulated proteins in the ATP synthase complex. This would be expected to manifest as a reduced ability to generate ATP yet no changes were observed in ATP synthase dependent oxygen consumption. The effects of DHA may not have been severe enough to observe at basal levels. Although maximal respiration is measured during the mito stress test, it is induced by uncoupling so may not be indicative of changes in ATP synthesis. Previous studies have observed that omega-3 fatty acids can alter mitochondrial function, altering ADP kinetics without altering maximal respiration (20). It remains to be seen if this reduction in ATP synthase proteins would alter the mitochondrial response to cellular stress or changing substrate availability.

In summary, we demonstrate that EPA and DHA display divergent metabolic activities in a skeletal muscle cell line, which may be partially mediated by differential remodelling of the lipidome. We speculate that the remodelling of the membrane-associated proteome is secondary to the changes observed in the saturation profile of the membrane-associated phospholipid species. Whilst the proteomic data did not reveal a mechanism for the effects of EPA on glucose uptake, our data support the proof of concept that a redistribution of the proteome may be responsible. Gene ontology analysis of the proteomic data indicate that the mechanism of action of EPA on protein metabolism may be driven by an improved fidelity with which proteins are synthesised. Based on the shifts in ribosomal proteins found in the membrane fractions future work should determine if EPA and DHA alter the transcript profiles in various ribosomal fractions.

References

1. **Aas V, Rokling-Andersen MH, Kase ET, Thoresen GH, and Rustan AC**. Eicosapentaenoic acid (20:5 n-3) increases fatty acid and glucose uptake in cultured human skeletal muscle cells. *J Lipid Res* 47: 366-374, 2006.
2. **Achard F, Benistant C, and Lagarde M**. Interconversions and distinct metabolic fate of eicosapentaenoic, docosapentaenoic and docosahexaenoic acids in bovine aortic endothelial cells. *Biochim Biophys Acta* 1255: 260-266, 1995.
3. **Akiba S, Murata T, Kitatani K, and Sato T**. Involvement of lipoxygenase pathway in docosapentaenoic acid-induced inhibition of platelet aggregation. *Biol Pharm Bull* 23: 1293-1297, 2000.
4. **Akinkuolie AO, Ngwa JS, Meigs JB, and Djousse L**. Omega-3 polyunsaturated fatty acid and insulin sensitivity: a meta-analysis of randomized controlled trials. *Clin Nutr* 30: 702-707, 2011.
5. **Alexander JW, Saito H, Trocki O, and Ogle CK**. The importance of lipid type in the diet after burn injury. *Ann Surg* 204: 1-8, 1986.
6. **Andersson A, Nalsen C, Tengblad S, and Vessby B**. Fatty acid composition of skeletal muscle reflects dietary fat composition in humans. *Am J Clin Nutr* 76: 1222-1229, 2002.
7. **Browning LM, Walker CG, Mander AP, West AL, Gambell J, Madden J, Calder PC, and Jebb SA**. Compared with daily, weekly n-3 PUFA intake affects the incorporation of eicosapentaenoic acid and docosahexaenoic acid into platelets and mononuclear cells in humans. *J Nutr* 144: 667-672, 2014.
8. **Burdge GC, and Calder PC**. Introduction to fatty acids and lipids. *World Rev Nutr Diet* 112: 1-16, 2015.
9. **Ciechanover A**. Intracellular protein degradation: from a vague idea thru the lysosome and the ubiquitin-proteasome system and onto human diseases and drug targeting. *Cell Death Differ* 12: 1178-1190, 2005.
10. **Cox J, and Mann M**. MaxQuant enables high peptide identification rates, individualized p.p.b.-range mass accuracies and proteome-wide protein quantification. *Nat Biotechnol* 26: 1367-1372, 2008.
11. **Cox J, Neuhauser N, Michalski A, Scheltema RA, Olsen JV, and Mann M**. Andromeda: a peptide search engine integrated into the MaxQuant environment. *J Proteome Res* 10: 1794-1805, 2011.
12. **Da Boit M, Sibson R, Sivasubramaniam S, Meakin JR, Greig CA, Aspden RM, Thies F, Jeromson S, Hamilton DL, Speakman JR, Hambly C, Mangoni AA, Preston T, and Gray SR**. Sex differences in the effect of fish oil supplementation on the adaptive response to resistance exercise training in older people: a randomized control trial. *Am J Clin Nutr* 2016.
13. **Dangardt F, Chen Y, Gronowitz E, Dahlgren J, Friberg P, and Strandvik B**. High physiological omega-3 Fatty Acid supplementation affects muscle Fatty Acid composition and glucose and insulin homeostasis in obese adolescents. *J Nutr Metab* 2012: 395757, 2012.
14. **Di Girolamo FG, Situlin R, Mazzucco S, Valentini R, Toigo G, and Biolo G**. Omega-3 fatty acids and protein metabolism: enhancement of anabolic interventions for sarcopenia. *Curr Opin Clin Nutr Metab Care* 17: 145-150, 2014.
15. **Ellgaard L, and Helenius A**. Quality control in the endoplasmic reticulum. *Nat Rev Mol Cell Biol* 4: 181-191, 2003.
16. **Findlay JA, Hamilton DL, and Ashford ML**. BACE1 activity impairs neuronal glucose oxidation: rescue by beta-hydroxybutyrate and lipoic acid. *Front Cell Neurosci* 9: 382, 2015.
17. **Folch J, Lees M, and Sloane Stanley GH**. A simple method for the isolation and purification of total lipides from animal tissues. *J Biol Chem* 226: 497-509, 1957.
18. **Franekova V, Angin Y, Hoebers NT, Coumans WA, Simons PJ, Glatz JF, Luiken JJ, and Larsen TS**. Marine omega-3 fatty acids prevent myocardial insulin resistance and metabolic remodeling as induced experimentally by high insulin exposure. *Am J Physiol Cell Physiol* 308: C297-307, 2015.

19. **Gregory MK, Gibson RA, Cook-Johnson RJ, Cleland LG, and James MJ**. Elongase reactions as control points in long-chain polyunsaturated fatty acid synthesis. *PLoS One* 6: e29662, 2011.
20. **Herbst EA, Paglialunga S, Gerling C, Whitfield J, Mukai K, Chabowski A, Heigenhauser GJ, Spriet LL, and Holloway GP**. Omega-3 supplementation alters mitochondrial membrane composition and respiration kinetics in human skeletal muscle. *J Physiol* 592: 1341-1352, 2014.
21. **Hessvik NP, Bakke SS, Fredriksson K, Boekschoten MV, Fjorkenstad A, Koster G, Hesselink MK, Kersten S, Kase ET, Rustan AC, and Thoresen GH**. Metabolic switching of human myotubes is improved by n-3 fatty acids. *J Lipid Res* 51: 2090-2104, 2010.
22. **Huang F, Wei H, Luo H, Jiang S, and Peng J**. EPA inhibits the inhibitor of kappaBalpha (IkappaBalpha)/NF-kappaB/muscle RING finger 1 pathway in C2C12 myotubes in a PPARgamma-dependent manner. *Br J Nutr* 105: 348-356, 2011.
23. **Jucker BM, Cline GW, Barucci N, and Shulman GI**. Differential effects of safflower oil versus fish oil feeding on insulin-stimulated glycogen synthesis, glycolysis, and pyruvate dehydrogenase flux in skeletal muscle: a 13C nuclear magnetic resonance study. *Diabetes* 48: 134-140, 1999.
24. **Kamolrat T, and Gray SR**. The effect of eicosapentaenoic and docosahexaenoic acid on protein synthesis and breakdown in murine C2C12 myotubes. *Biochem Biophys Res Commun* 432: 593-598, 2013.
25. **Kanayasu-Toyoda T, Morita I, and Murota S**. Docosapentaenoic acid (22:5, n-3), an elongation metabolite of eicosapentaenoic acid (20:5, n-3), is a potent stimulator of endothelial cell migration on pretreatment in vitro. *Prostaglandins Leukot Essent Fatty Acids* 54: 319-325, 1996.
26. **Kaur G, Sinclair AJ, Cameron-Smith D, Barr DP, Molero-Navajas JC, and Konstantopoulos N**. Docosapentaenoic acid (22:5n-3) down-regulates the expression of genes involved in fat synthesis in liver cells. *Prostaglandins Leukot Essent Fatty Acids* 85: 155-161, 2011.
27. **Lamaziere A, Wolf C, Barbe U, Bausero P, and Visioli F**. Lipidomics of hepatic lipogenesis inhibition by omega 3 fatty acids. *Prostaglandins Leukot Essent Fatty Acids* 88: 149-154, 2013.
28. **Lanza IR, Blachnio-Zabielska A, Johnson ML, Schimke JM, Jakaitis DR, Lebrasseur NK, Jensen MD, Sreekumaran Nair K, and Zabielski P**. Influence of fish oil on skeletal muscle mitochondrial energetics and lipid metabolites during high-fat diet. *Am J Physiol Endocrinol Metab* 304: E1391-1403, 2013.
29. **Magee P, Pearson S, Whittingham-Dowd J, and Allen J**. PPARgamma as a molecular target of EPA anti-inflammatory activity during TNF-alpha-impaired skeletal muscle cell differentiation. *J Nutr Biochem* 23: 1440-1448, 2012.
30. **McGlory C, Galloway SD, Hamilton DL, McClintock C, Breen L, Dick JR, Bell JG, and Tipton KD**. Temporal changes in human skeletal muscle and blood lipid composition with fish oil supplementation. *Prostaglandins Leukot Essent Fatty Acids* 90: 199-206, 2014.
31. **Mori TA, Burke V, Puddey IB, Watts GF, O'Neal DN, Best JD, and Beilin LJ**. Purified eicosapentaenoic and docosahexaenoic acids have differential effects on serum lipids and lipoproteins, LDL particle size, glucose, and insulin in mildly hyperlipidemic men. *Am J Clin Nutr* 71: 1085-1094, 2000.
32. **Mori TA, Codde JP, Vandongen R, and Beilin LJ**. New findings in the fatty acid composition of individual platelet phospholipids in man after dietary fish oil supplementation. *Lipids* 22: 744-750, 1987.
33. **Morisaki N, Kanzaki T, Fujiyama Y, Osawa I, Shirai K, Matsuoka N, Saito Y, and Yoshida S**. Metabolism of n-3 polyunsaturated fatty acids and modification of phospholipids in cultured rabbit aortic smooth muscle cells. *J Lipid Res* 26: 930-939, 1985.
34. **Murphy RA, Mourtzakis M, and Mazurak VC**. n-3 polyunsaturated fatty acids: the potential role for supplementation in cancer. *Curr Opin Clin Nutr Metab Care* 15: 246-251, 2012.
35. **Neschen S, Morino K, Dong J, Wang-Fischer Y, Cline GW, Romanelli AJ, Rossbacher JC, Moore IK, Regittnig W, Munoz DS, Kim JH, and Shulman GI**. n-3 Fatty acids preserve insulin sensitivity in vivo in a peroxisome proliferator-activated receptor-alpha-dependent manner. *Diabetes* 56: 1034-1041, 2007.

36. **Norris PC, and Dennis EA**. Omega-3 fatty acids cause dramatic changes in TLR4 and purinergic eicosanoid signaling. *Proc Natl Acad Sci U S A* 109: 8517-8522, 2012.
37. **Oh DY, Talukdar S, Bae EJ, Imamura T, Morinaga H, Fan W, Li P, Lu WJ, Watkins SM, and Olefsky JM**. GPR120 is an omega-3 fatty acid receptor mediating potent anti-inflammatory and insulin-sensitizing effects. *Cell* 142: 687-698, 2010.
38. **Ong SE, Blagoev B, Kratchmarova I, Kristensen DB, Steen H, Pandey A, and Mann M**. Stable isotope labeling by amino acids in cell culture, SILAC, as a simple and accurate approach to expression proteomics. *Mol Cell Proteomics* 1: 376-386, 2002.
39. **Ries A, Trottenberg P, Elsner F, Stiel S, Haugen D, Kaasa S, and Radbruch L**. A systematic review on the role of fish oil for the treatment of cachexia in advanced cancer: an EPCRC cachexia guidelines project. *Palliative medicine* 26: 294-304, 2012.
40. **Rodacki CL, Rodacki AL, Pereira G, Naliwaiko K, Coelho I, Pequito D, and Fernandes LC**. Fish-oil supplementation enhances the effects of strength training in elderly women. *Am J Clin Nutr* 95: 428-436, 2012.
41. **Ron D**. Translational control in the endoplasmic reticulum stress response. *The Journal of Clinical Investigation* 110: 1383-1388, 2002.
42. **Sjovall P, Rossmeisl M, Hanrieder J, Kuda O, Kopecky J, and Bryhn M**. Dietary uptake of omega-3 fatty acids in mouse tissue studied by time-of-flight secondary ion mass spectrometry (TOF-SIMS). *Anal Bioanal Chem* 407: 5101-5111, 2015.
43. **Smith GI, Atherton P, Reeds DN, Mohammed BS, Rankin D, Rennie MJ, and Mittendorfer B**. Dietary omega-3 fatty acid supplementation increases the rate of muscle protein synthesis in older adults: a randomized controlled trial. *Am J Clin Nutr* 93: 402-412, 2011.
44. **Smith GI, Atherton P, Reeds DN, Mohammed BS, Rankin D, Rennie MJ, and Mittendorfer B**. Omega-3 polyunsaturated fatty acids augment the muscle protein anabolic response to hyperinsulinaemia-hyperaminoacidaemia in healthy young and middle-aged men and women. *Clin Sci (Lond)* 121: 267-278, 2011.
45. **Smith GI, Julliand S, Reeds DN, Sinacore DR, Klein S, and Mittendorfer B**. Fish oil-derived n-3 PUFA therapy increases muscle mass and function in healthy older adults. *Am J Clin Nutr* 102: 115-122, 2015.
46. **Stephens FB, Mendis B, Shannon CE, Cooper S, Ortori CA, Barrett DA, Mansell P, and Tsintzas K**. Fish oil omega-3 fatty acids partially prevent lipid-induced insulin resistance in human skeletal muscle without limiting acylcarnitine accumulation. *Clin Sci (Lond)* 127: 315-322, 2014.
47. **Storlien LH, Jenkins AB, Chisholm DJ, Pascoe WS, Khouri S, and Kraegen EW**. Influence of dietary fat composition on development of insulin resistance in rats. Relationship to muscle triglyceride and omega-3 fatty acids in muscle phospholipid. *Diabetes* 40: 280-289, 1991.
48. **Storlien LH, Kraegen EW, Chisholm DJ, Ford GL, Bruce DG, and Pascoe WS**. Fish oil prevents insulin resistance induced by high-fat feeding in rats. *Science* 237: 885-888, 1987.
49. **Tripathi R, Benz N, Culleton B, Trouve P, and Ferec C**. Biophysical characterisation of calumenin as a charged F508del-CFTR folding modulator. *PLoS One* 9: e104970, 2014.
50. **Vance JE**. Phospholipid synthesis and transport in mammalian cells. *Traffic* 16: 1-18, 2015.
51. **Vance JE, and Tasseva G**. Formation and function of phosphatidylserine and phosphatidylethanolamine in mammalian cells. *Biochim Biophys Acta* 1831: 543-554, 2013.
52. **Wang Y, Lin QW, Zheng PP, Zhang JS, and Huang FR**. DHA inhibits protein degradation more efficiently than EPA by regulating the PPARgamma/NFkappaB pathway in C2C12 myotubes. *Biomed Res Int* 2013: 318981, 2013.
53. **Woodman RJ, Mori TA, Burke V, Puddey IB, Watts GF, Best JD, and Beilin LJ**. Docosahexaenoic acid but not eicosapentaenoic acid increases LDL particle size in treated hypertensive type 2 diabetic patients. *Diabetes Care* 26: 253, 2003.
54. **Yea K, Kim J, Yoon JH, Kwon T, Kim JH, Lee BD, Lee HJ, Lee SJ, Kim JI, Lee TG, Baek MC, Park HS, Park KS, Ohba M, Suh PG, and Ryu SH**. Lysophosphatidylcholine activates adipocyte glucose

749 uptake and lowers blood glucose levels in murine models of diabetes. *J Biol Chem* 284: 33833-33840,
750 2009.
751 55. **You JS, Park MN, Song W, and Lee YS**. Dietary fish oil alleviates soleus atrophy during
752 immobilization in association with Akt signaling to p70s6k and E3 ubiquitin ligases in rats. *Appl*
753 *Physiol Nutr Metab* 35: 310-318, 2010.

754

755 ACKNOWLEDGEMENTS

756 This work was funded by a University of Stirling capital investment award (DLH) and Society for
757 Endocrinology and American College of Sports Medicine early career awards (DLH). The financial
758 support of Highlands and Islands Enterprise, Scottish Funding Council and European Regional
759 Development Fund is gratefully acknowledged (IM, MKD and PDW). We acknowledge Liz
760 Mackinlay for assistance with the FAME analysis.

761

762 **Figure Legends**

763 **Figure 1. EPA and DHA enhance n-3 content to a similar degree.** C_2C_{12} myotubes were incubated
764 in either fatty acid free 2% BSA or fatty acid free 2% BSA pre-conjugated to 50 μM EPA or 50 μM
765 DHA for 72hrs. Fatty acid analysis was carried out by FAME analysis (n=4 in duplicate) and data are
766 presented as % change from BSA control grouped by fatty acid species; SFA – saturated fatty acids,
767 MUFA – monounsaturated fatty acids, n-9 PUFA – omega-9 polyunsaturated fatty acids, n-6 PUFA –
768 omega-6 polyunsaturated fatty acids, n-3 PUFA – omega-3 polyunsaturated fatty acids.

769 **Figure 2. EPA and DHA have differential effects on C_2C_{12} glucose uptake independently of**
770 **changes in PKB Thr308 phosphorylation or GLUT1/4 and Hexokinase1/2 expression.** Glucose
771 uptake was determined using a radiolabelled 2 Deoxy-glucose uptake assay (n=6 in duplicate) (A) and
772 PKB Thr308 phosphorylation (n=4 in duplicate) (B) was determined using SDS-PAGE and phospho-
773 specific antibodies, the signal for which was normalised to t-PKB expression (representative blots are
774 inset). GLUT1/4 expression (C) were normalised to t-eEF2 whilst Hexokinase1/2 expression (D) were
775 normalised to α-tubulin. Bars not connected by the same letter are significantly different from each
776 other ($p<0.05$).

777 **Figure 3. EPA and DHA treatment do not modulate mitochondrial function or mitochondrial**
778 **protein expression.** C_2C_{12} myotubes were incubated in either fatty acid free 2% BSA or fatty acid
779 free 2% BSA pre-conjugated to 50 μM EPA or 50 μM DHA for 48hrs. One set of myotubes was
780 exposed to a mitochondrial stress test in the SeaHorse XFA and oxygen consumption was assessed
781 (A). A parallel set of myotubes were collected for western blot analysis of mitochondrial protein
782 expression with the mito-blot panel (B). Representative blots are shown in (C).

783 **Figure 4. EPA enhances protein accretion through a reduction in protein breakdown.** A) Protein
784 synthesis was measured by a L-[2,4,^{3}H] phenylalanine incorporation assay following a 24 hr
785 incubation with n-3 fatty acids (n=5 in duplicate) B) protein breakdown was assessed by the release of
786 L-[2,4,^{3}H] phenylalanine into culture media after 24hr treatment with n-3 fatty acids (n=10, in
787 duplicate) C) total protein content was assessed after a 72hr incubation with EPA or DHA (n=5, in

duplicate) D) Phosphorylation of proteins within the mTOR signalling pathway were assessed by western blotting after a 24 hr incubation with n-3 fatty acids (n=3 in duplicate) E) ubiquitination of proteins were assessed by western blotting after a 24hr incubation with fatty acids (n=3 in duplicate). # indicates significantly different from Veh and DHA, * indicates significantly different from corresponding control condition ($p<0.05$).

Figure 5. Complete fatty acid profiles reveal a number of fatty acids differentially regulated by EPA and DHA. C_2C_{12} myotubes were incubated in either fatty acid free 2% BSA or fatty acid free 2% BSA pre-conjugated to 50 μM EPA or 50 μM DHA for 72hrs (n=4 in duplicate). Cells were pelleted and washed 3x using PBS with 2% fatty acid free BSA. Fatty acid analysis was carried out by FAME analysis. The fold change was determined from the BSA control condition and logged (log2). ND indicates non detectable, * indicates significant difference between EPA vs DHA ($p<0.05$).

Figure 6. Global lipidomic analysis characterises shifts in lipid composition of C_2C_{12} myotubes. Principal component analysis (PCA) scores plots of lipid profiles generated by LC-MS in (A) positive ion and (B) negative ion modes. Cultured cells were incubated with either fatty acid free 2% BSA (green circles), fatty acid free 2% BSA pre-conjugated to 50 μM EPA (red triangles) or 50 μM DHA (blue squares) for 72hrs. Global lipidomic analysis was performed on the cells and the data sets were subjected to PCA with Pareto scaling. Each point represents a single cell sample (n=6). The PCA revealed that the control, EPA and DHA groups could be discriminated on the basis of their lipid profiles. The control cells were found to cluster in one area of the scores plot whilst cells treated with EPA or DHA appeared in regions away from the controls indicating that were alterations in their lipid composition as a result of the fatty acid treatments.

Figure 7. Lipidomic profiling reveals cellular lipid species containing EPA, DPA and DHA. Positive ion orthogonal partial least-squares discriminant analysis (OPLS-DA) for (A) BSA vs DHA and (B) BSA vs EPA (n=6). Green circles indicate BSA treated C_2C_{12} myotubes; blue squares indicate DHA treated C_2C_{12} myotubes and red triangles indicate EPA treated C_2C_{12} myotubes. The OPLS-DA scores plots indicated that EPA and DHA groups had distinct lipid profiles compared to the controls. In order to determine the lipids responsible for the inter-class differences associated S-plots of

covariance versus the correlation were generated. Each point in the S-plots represents a lipid detected in the LC-MS analysis with the lipids at the top and bottom of the plots showing the greatest changes. The analysis revealed that there was a relative increase in the abundance of lipid species containing 20:5, 22:5 or 22:6 fatty acids in EPA and DHA treated cells respectively.

Figure 8. Targeted phospholipid analysis indicates preferential incorporation of long chain polyunsaturated fatty acids into specific phospholipid classes. C_2C_{12} myotubes were solvent extracted and molecular species of (A) phosphatidylcholine and (B) phosphatidylethanolamines were detected by ESI-MS/MS in positive-ion mode by means of a precursor ion scan for m/z 184 and a neutral loss scan of m/z 141 respectively.

Figure 9. Targeted phospholipid analysis presented as % abundance for PC, PE, LPC and LPE species. C_2C_{12} myotubes were solvent extracted and molecular species of (A) lyso-phosphatidylcholine, (B) phosphatidylcholine, (C) lyso-phosphatidylethanolamine and (D) phosphatidylethanolamine were detected by ESI-MS/MS in positive-ion mode by means of a precursor ion scan for m/z 184 and a neutral loss scan of m/z 141 respectively. Data are presented as % abundance ± SEM. Bars not connected by the same letter are significantly different from one another ($p<0.05$).

Figure 10. Membrane associated proteomics reveals protein folding machinery and ribosomal proteins differentially shift to the membrane in response to EPA treatment. C_2C_{12} myotubes were incubated in SILAC media for 7 doublings followed by plating and differentiation for 72hrs in SILAC differentiation media. Following differentiation myotubes were incubated in either fatty acid free 2% BSA or fatty acid free 2% BSA pre-conjugated to 50 μM EPA or 50 μM DHA for 72hrs (n=3 in duplicate). Cells were collected and fractionated, the membrane fraction was then submitted to proteomics analysis. (A) Venne diagram illustrating the number of proteins found to be changed in the membrane fraction in response to EPA/DHA. (B) String diagram illustrating the interactions between the proteins identified from the GO analysis as being involved in 'protein folding.' (C) Fold change in

841 ribosomal proteins in the membrane fraction in response to EPA/DHA. * indicates a significant fold
842 change from control ($p<0.05$). All differences between EPA and DHA were significant.

843

844

845

846

847

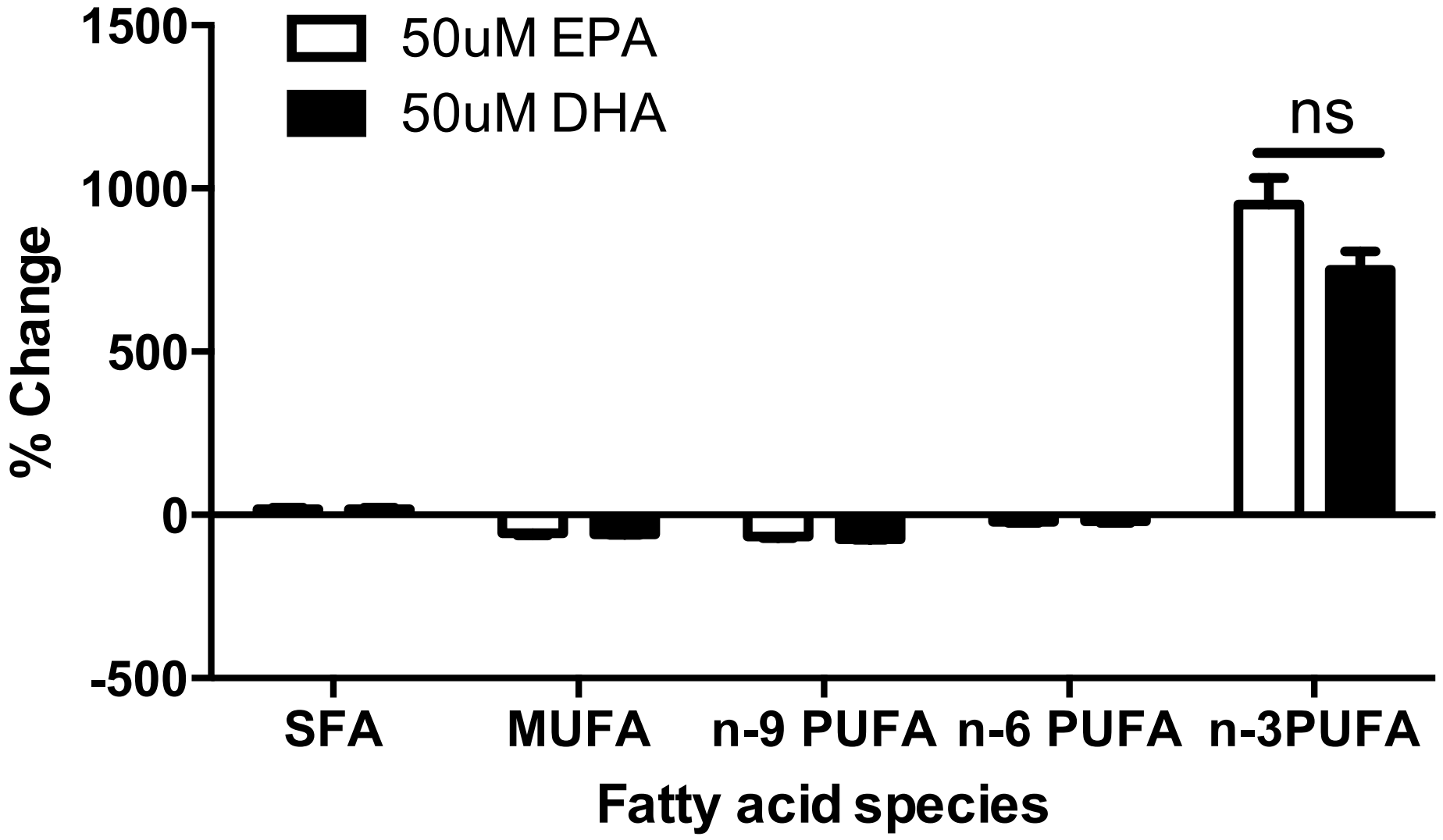
50uM EPA
50uM DHA
ns
1500
1000
500
0
-500
% Change
SFA
MUFA
n-9 PUFA
n-6 PUFA
n-3PUFA
Fatty acid species

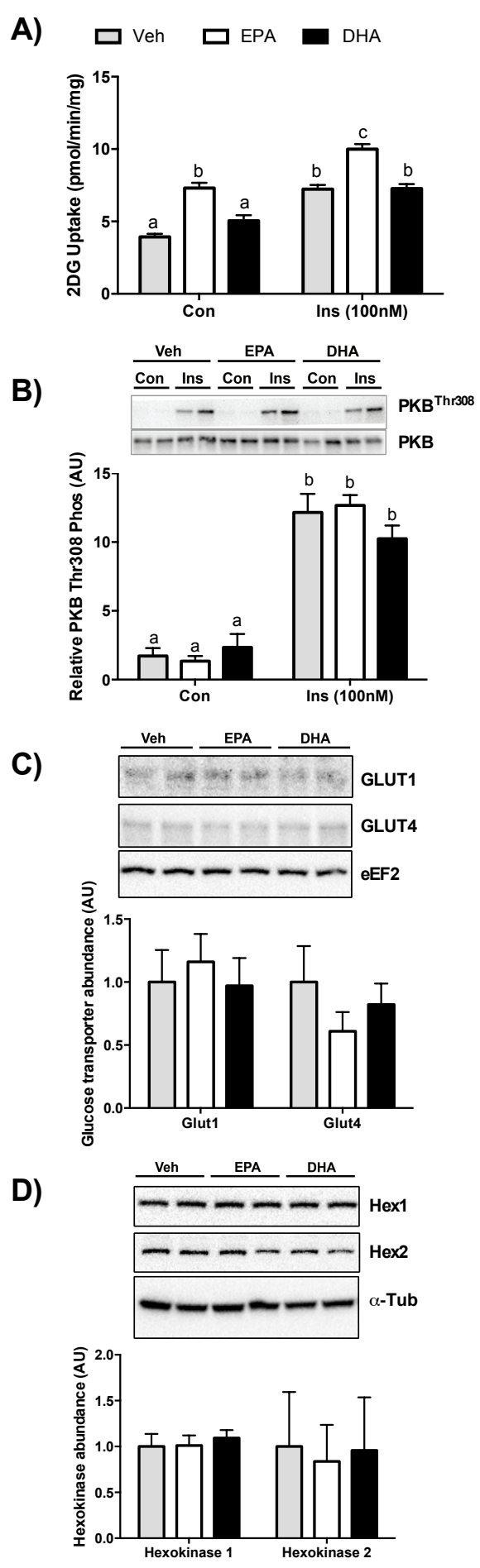
A)
Veh
EPA
DHA
2DG Uptake (pmol/min/mg)
15
10
5
0
a
b
a
b
c
b
Con
Ins (100nM)
B)
Veh
EPA
DHA
Con
Ins
Con
Ins
Con
Ins
PKB Thr308
PKB
Relative PKB Thr308 Phos (AU)
15
10
5
0
a
a
a
b
b
b
Con
Ins (100nM)
C)
Veh
EPA
DHA
GLUT1
GLUT4
eEF2
Glucose transporter abundance (AU)
1.5
1.0
0.5
0.0
Glut1
Glut4
D)
Veh
EPA
DHA
Hex1
Hex2
α-Tub
Hexokinase abundance (AU)
2.0
1.5
1.0
0.5
0.0
Hexokinase 1
Hexokinase 2

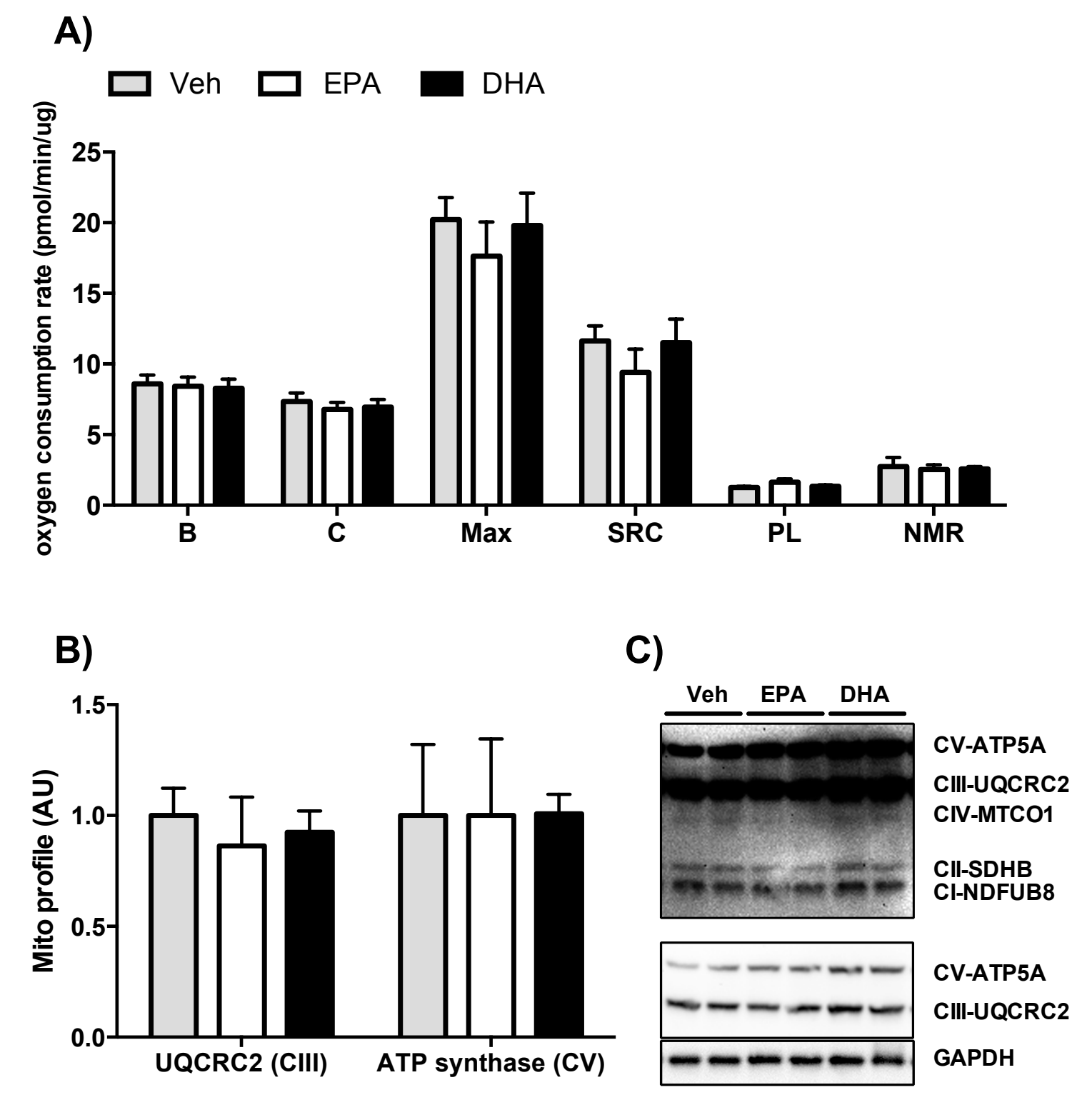
A)
Veh
EPA
DHA
oxygen consumption rate (pmol/min/ug)
25
20
15
10
5
0
B
C
Max
SRC
PL
NMR
B)
Mito profile (AU)
1.5
1.0
0.5
0.0
UQCRC2 (CIII)
ATP synthase (CV)
C)
Veh
EPA
DHA
CV-ATP5A
CIII-UQCRC2
CIV-MTCO1
CII-SDHB
CI-NDFUB8
CV-ATP5A
CIII-UQCRC2
GAPDH

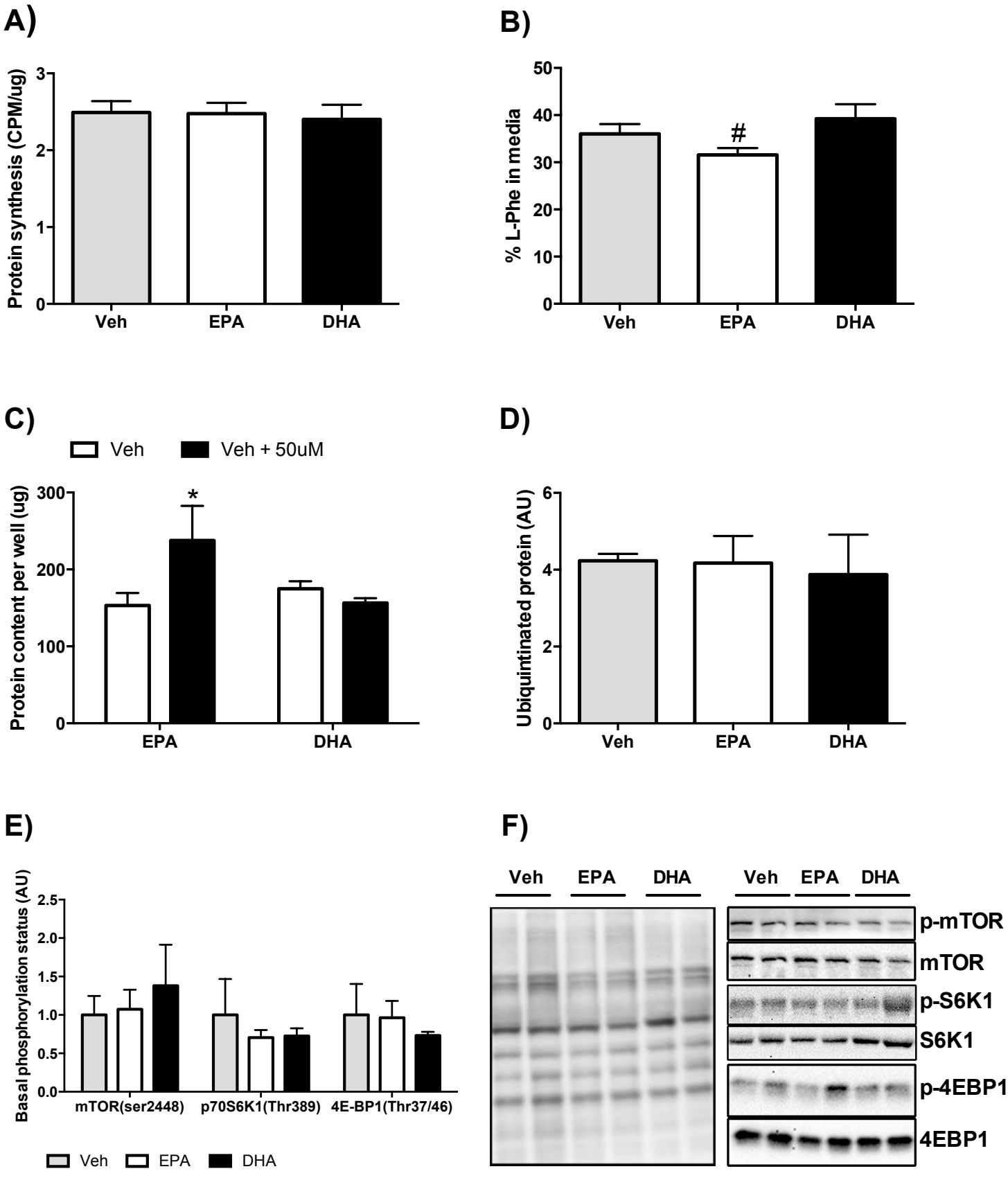
A)
Protein synthesis (CPM/ug)
3
2
1
0
Veh
EPA
DHA
B)
% L-Phe in media
50
40
30
20
10
0
#
Veh
EPA
DHA
C)
Veh
Veh + 50uM
Protein content per well (ug)
300
200
100
0
*
EPA
DHA
D)
Ubiquintinated protein (AU)
6
4
2
0
Veh
EPA
DHA
E)
Basal phosphorylation status (AU)
2.5
2.0
1.5
1.0
0.5
0.0
mTOR(ser2448)
p70S6K1(Thr389)
4E-BP1(Thr37/46)
Veh
EPA
DHA
F)
Veh
EPA
DHA
Veh
EPA
DHA
p-mTOR
mTOR
p-S6K1
S6K1
p-4EBP1
4EBP1

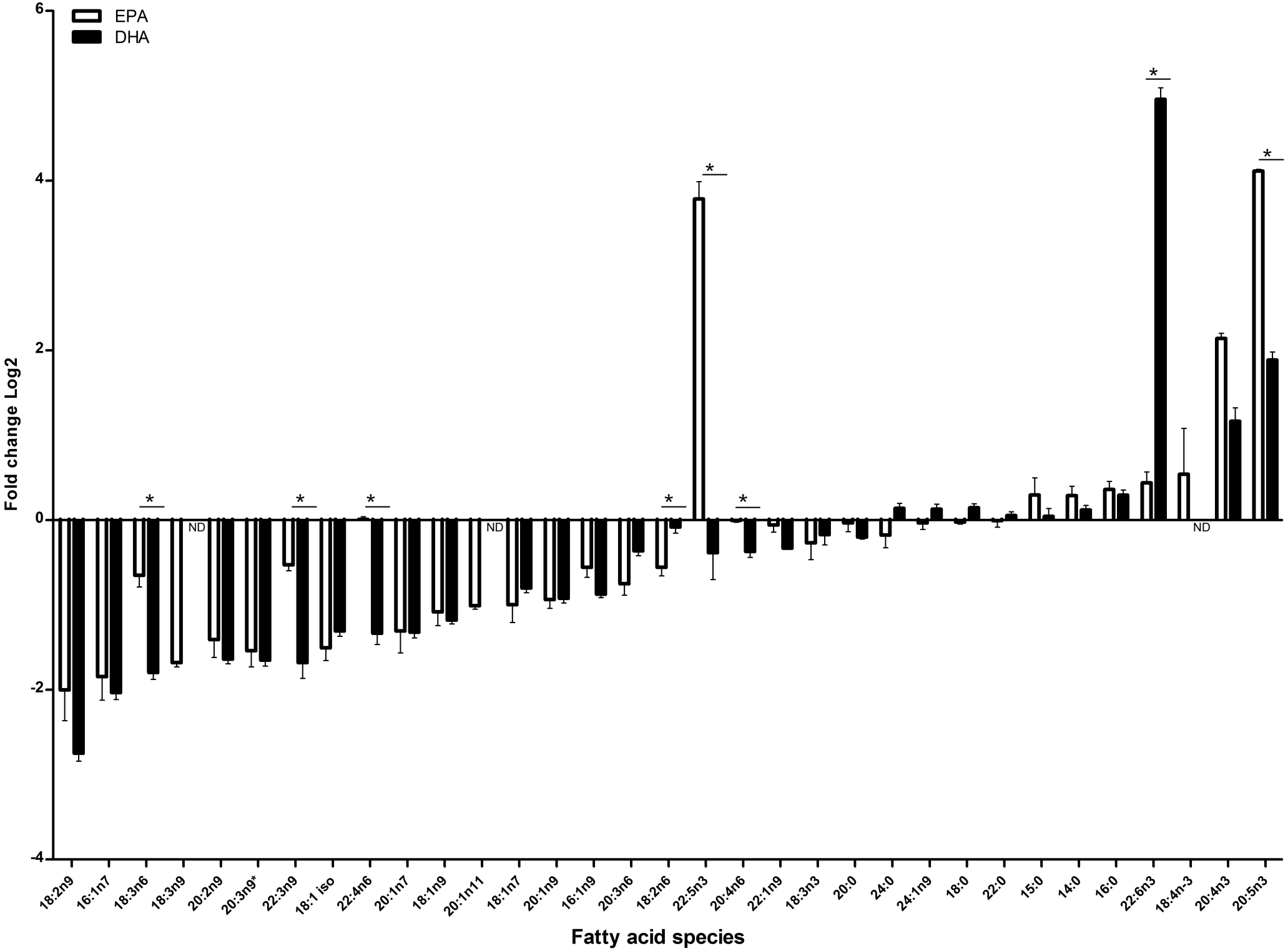
EPA
DHA
6
4
2
0
-2
-4
Fold change Log2
*
ND
18:2n9
16:1n7
18:3n6
18:3n9
20:2n9
20:3n9*
22:3n9
18:1 iso
22:4n6
20:1n7
18:1n9
20:1n11
18:1n7
20:1n9
16:1n9
20:3n6
18:2n6
22:5n3
20:4n6
22:1n9
18:3n3
20:0
24:0
24:1n9
18:0
22:0
15:0
14:0
16:0
22:6n3
18:4n-3
20:4n3
20:5n3
Fatty acid species

A)

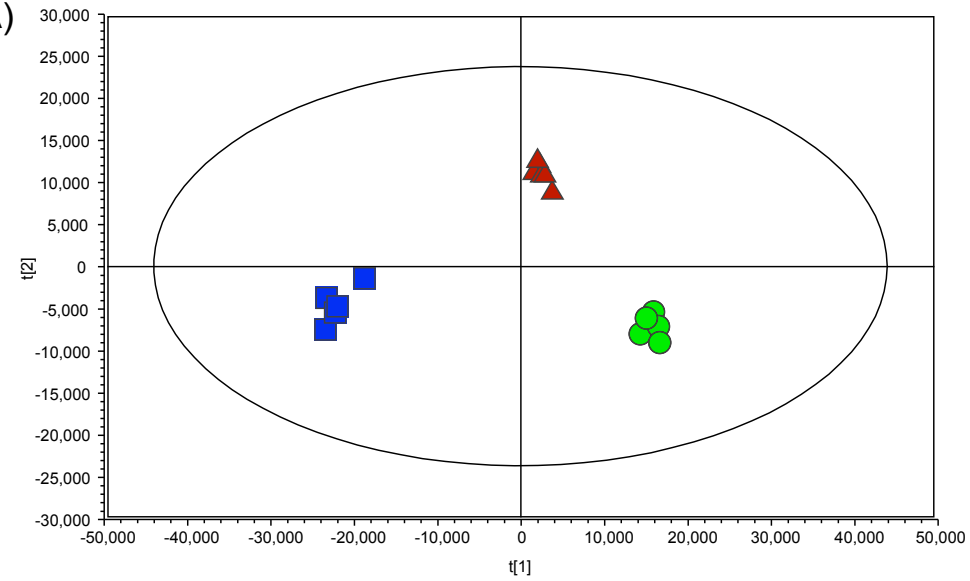
30,000
25,000
20,000
15,000
10,000
5,000
0
-5,000
-10,000
-15,000
-20,000
-25,000
-30,000
t[2]
-50,000
-40,000
-30,000
-20,000
-10,000
0
10,000
20,000
30,000
40,000
50,000
t[1]

B)

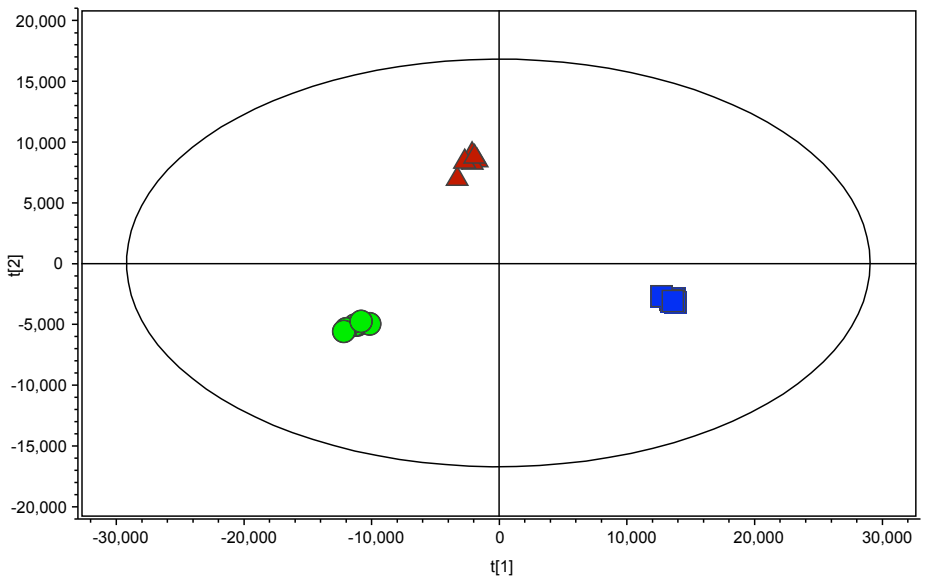
20,000
15,000
10,000
5,000
0
-5,000
-10,000
-15,000
-20,000
t[2]
-30,000
-20,000
-10,000
0
10,000
20,000
30,000
t[1]

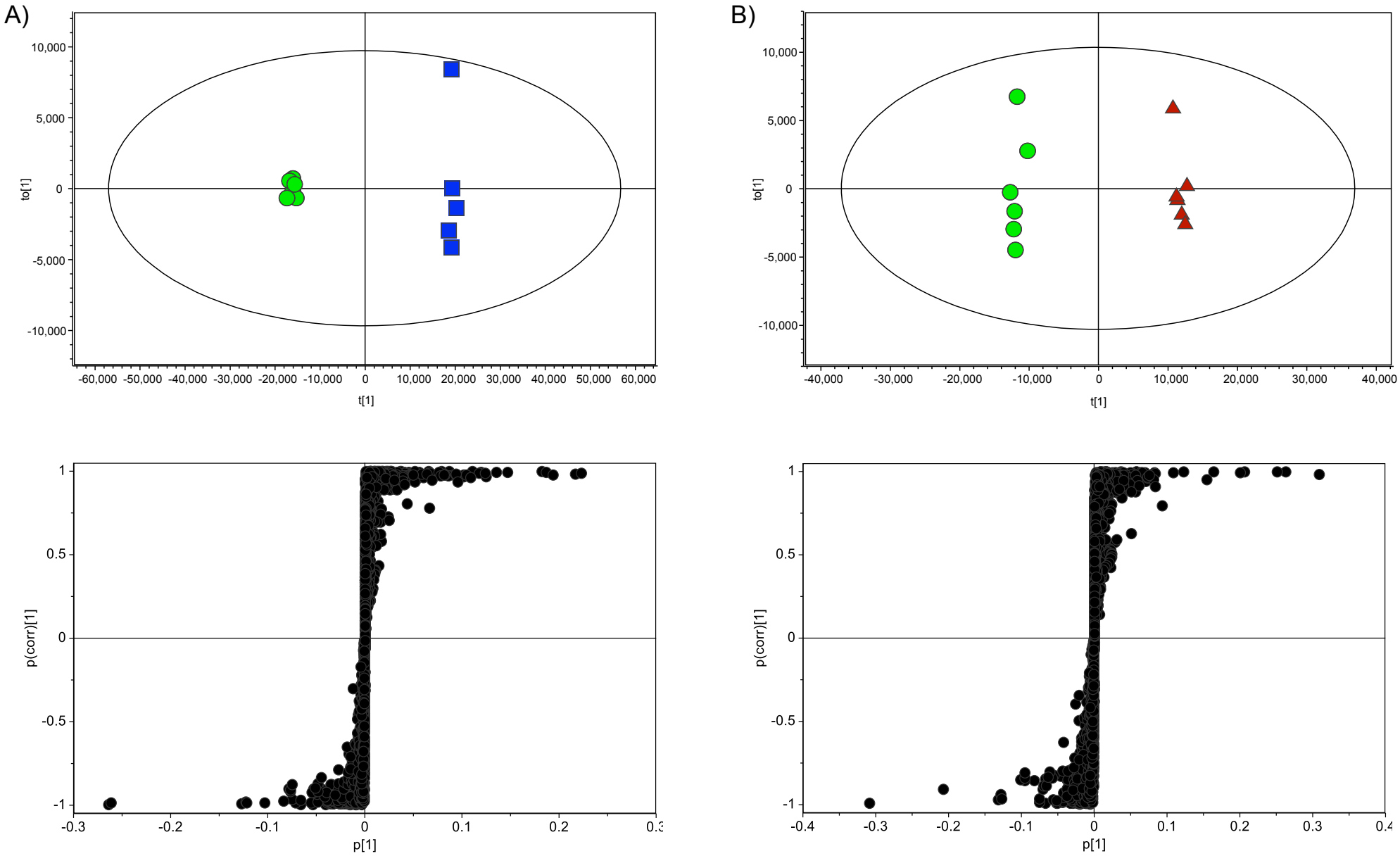
A)
B)
to[1]
t[1]
p(corr)[1]
p[1]

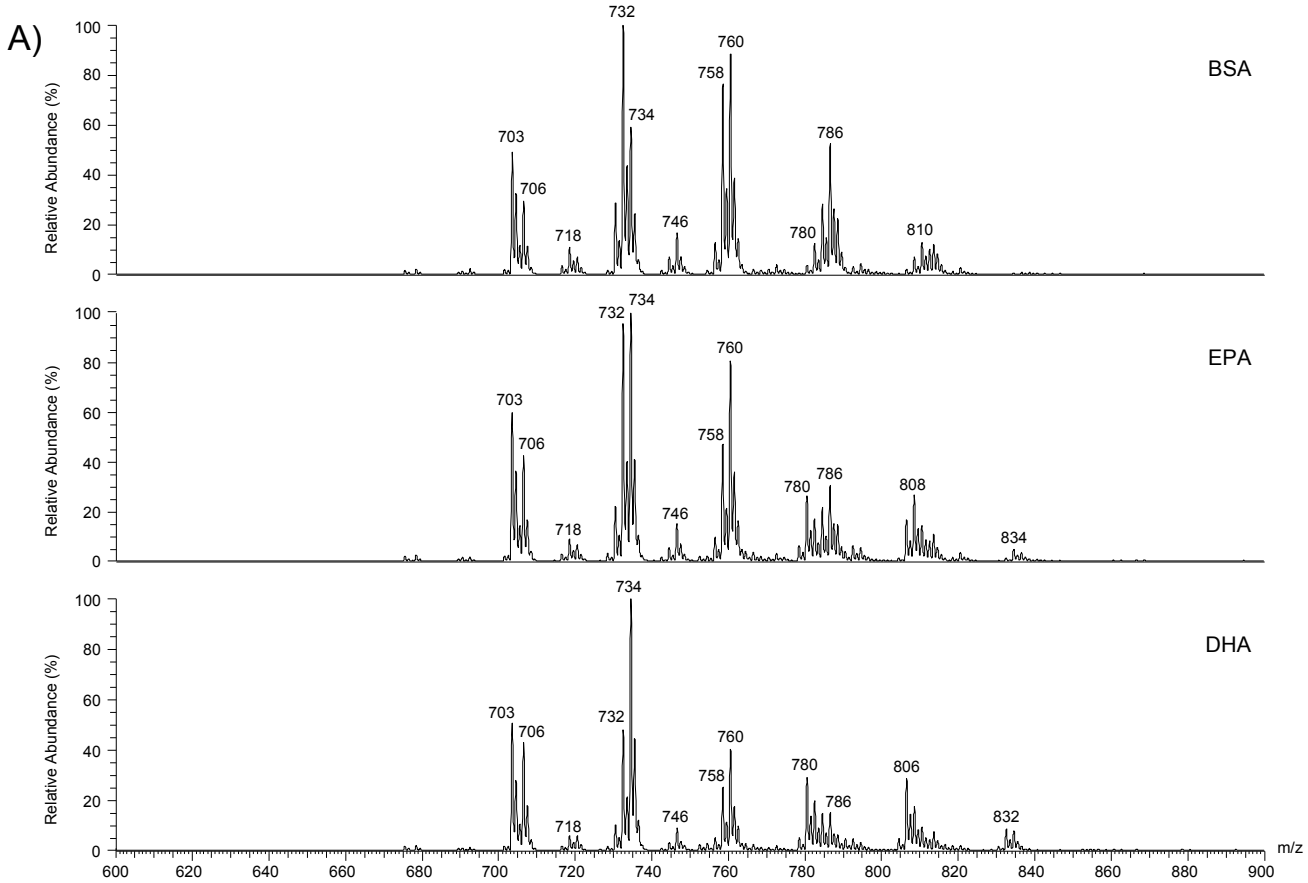
A)
BSA
EPA
DHA
Relative Abundance (%)
m/z
732
760
758
734
703
706
786
718
746
780
810
732
734
760
703
706
758
780
786
808
718
746
834
734
703
732
706
760
758
780
806
786
718
746
832
600
620
640
660
680
700
720
740
760
780
800
820
840
860
880
900

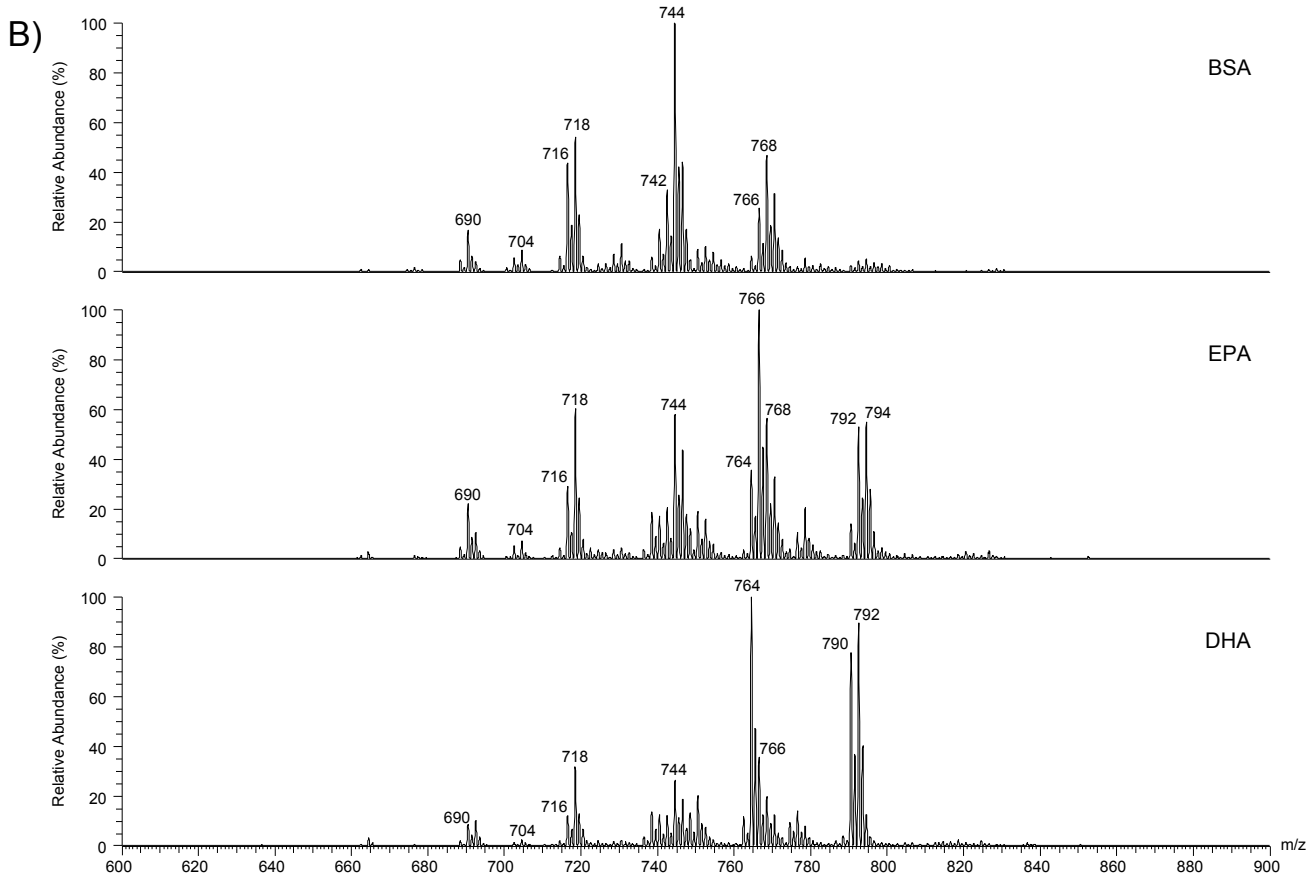
B)
BSA
EPA
DHA
Relative Abundance (%)
m/z
744
718
716
768
742
766
690
704
766
718
744
768
792
794
764
716
690
704
764
792
790
766
718
744
716
690
704
600
620
640
660
680
700
720
740
760
780
800
820
840
860
880
900

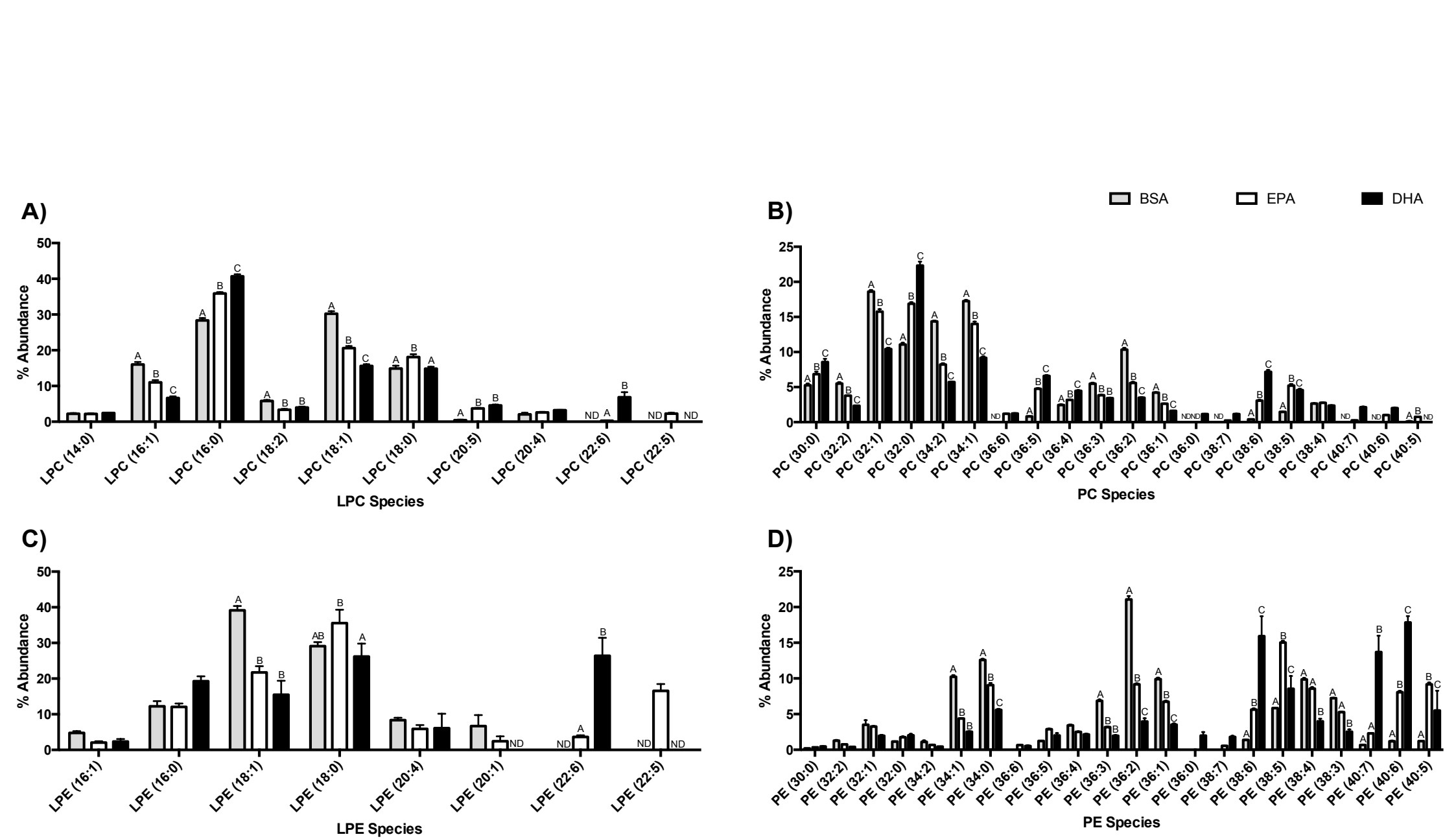
A)
B)
C)
D)
BSA
EPA
DHA
% Abundance
LPC Species
LPC (14:0)
LPC (16:1)
LPC (16:0)
LPC (18:2)
LPC (18:1)
LPC (18:0)
LPC (20:5)
LPC (20:4)
LPC (22:6)
LPC (22:5)
PC Species
PC (30:0)
PC (32:2)
PC (32:1)
PC (32:0)
PC (34:2)
PC (34:1)
PC (36:6)
PC (36:5)
PC (36:4)
PC (36:3)
PC (36:2)
PC (36:1)
PC (36:0)
PC (38:7)
PC (38:6)
PC (38:5)
PC (38:4)
PC (40:7)
PC (40:6)
PC (40:5)
LPE Species
LPE (16:1)
LPE (16:0)
LPE (18:1)
LPE (18:0)
LPE (20:4)
LPE (20:1)
LPE (22:6)
LPE (22:5)
PE Species
PE (30:0)
PE (32:2)
PE (32:1)
PE (32:0)
PE (34:2)
PE (34:1)
PE (34:0)
PE (36:6)
PE (36:5)
PE (36:4)
PE (36:3)
PE (36:2)
PE (36:1)
PE (36:0)
PE (38:7)
PE (38:6)
PE (38:5)
PE (38:4)
PE (38:3)
PE (40:7)
PE (40:6)
PE (40:5)
ND

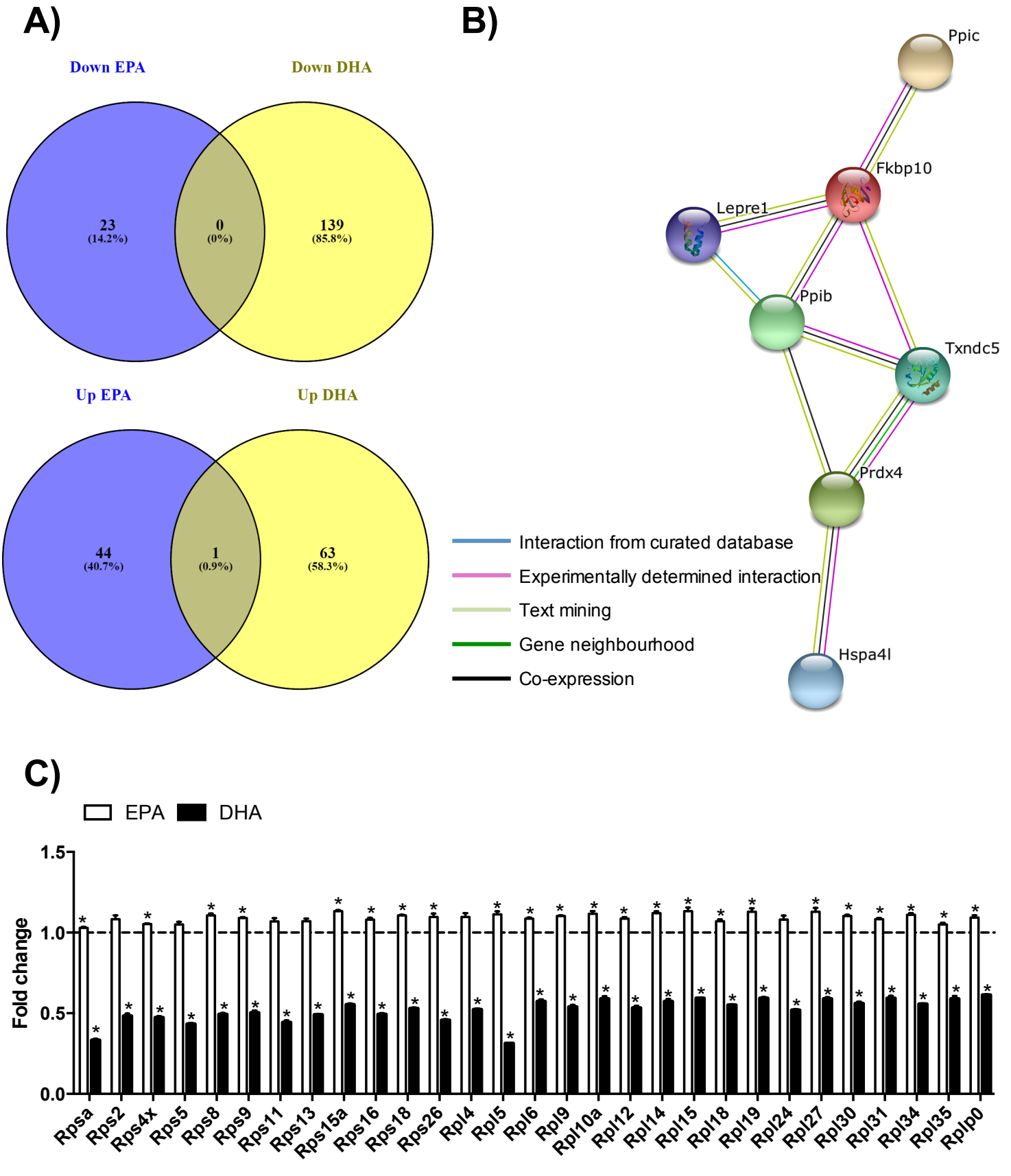
A)
Down EPA
Down DHA
23
(14.2%)
0
(0%)
139
(85.8%)
Up EPA
Up DHA
44
(40.7%)
1
(0.9%)
63
(58.3%)
B)
Ppic
Fkbp10
Lepre1
Ppib
Txndc5
Prdx4
Hspa4l
Interaction from curated database
Experimentally determined interaction
Text mining
Gene neighbourhood
Co-expression
C)
EPA
DHA
Fold change
1.5
1.0
0.5
0.0
Rpsa
Rps2
Rps4x
Rps5
Rps8
Rps9
Rps11
Rps13
Rps15a
Rps16
Rps18
Rps26
Rpl4
Rpl5
Rpl6
Rpl9
Rpl10a
Rpl12
Rpl14
Rpl15
Rpl18
Rpl19
Rpl24
Rpl27
Rpl30
Rpl31
Rpl34
Rpl35
Rplp0